

WANG, HONGZHOU Ph.D. Exploring Alternative Mass Spectrometric Methods For Epitranscriptomic analysis. (2022)
Directed by Dr. Norman H.L. Chiu. 68p.

Ribonucleic acid (RNA) is one of the key components in living cells and plays many different roles. For example, RNA can be the cornerstone of biological function, in particular, it can be catalytic, and thus possess both a genotype and a phenotype.¹ In order to achieve some of the RNA functionalities, the molecular structure of RNA can be altered by a whole spectrum of post-transcriptional modifications. Those modifications refer mainly to the changes in the molecular structure of ribonucleotides. Currently, there are 172 different RNA modifications reported in the literature.² Among them, the most frequent modification is RNA methylation.^{3,4} With the advances in the annotation of genomes, there are growing interests to analyze the RNA modifications at the transcriptomic level.^{5,6,7,8,9,10} In the literature, this area of research is referred as epitranscriptomic analysis. The goal of epitranscriptomic analysis is to determine the identity and frequency of all RNA modifications in a specific transcriptome, and ultimately pinpointing their exact locations on each transcript. Currently, the most suitable and comprehensive approach

¹ Lehman, "RNA in Evolution."

² Boccaletto et al., "MODOMICS: A Database of RNA Modification Pathways. 2017 Update."

³ Zaccara, Ries, and Jaffrey, "Reading, Writing and Erasing mRNA Methylation."

⁴ Shi, Wei, and He, "Where, When, and How: Context-Dependent Functions of RNA Methylation Writers, Readers, and Erasers."

⁵ Licht and Jantsch, "Rapid and Dynamic Transcriptome Regulation by RNA Editing and RNA Modifications."

⁶ Basanta-Sanchez et al., "Attomole Quantification and Global Profile of RNA Modifications: Epitranscriptome of Human Neural Stem Cells."

⁷ Nachtergaele and He, "Chemical Modifications in the Life of an mRNA Transcript."

⁸ Pan, "Modifications and Functional Genomics of Human Transfer RNA."

⁹ Huber et al., "The Versatile Roles of the tRNA Epitranscriptome during Cellular Responses to Toxic Exposures and Environmental Stress."

¹⁰ Konno, Taniguchi, and Ishii, "Significant Epitranscriptomes in Heterogeneous Cancer."

for carrying out epitranscriptomic analysis is using liquid chromatography mass spectrometry (LC-MS) method to analyze the digested ribonucleosides.^{6,9,11,12} Our research group have recently developed a novel and accurate LC-MS/MS method which could achieve standard-free profiling and quantitation for modified ribonucleosides. Aiming at further improve or assist the LC-MS/MS method, alternative mass spectrometric methods are present in this dissertation. These include a size reducing ion mobility (SRI) mass spectrometric method and a flow injection analysis (FIA) method which can improve the differentiation and turnaround time of targeted analysis, respectively.

¹¹ Collin and Limbach, “Mass Spectrometry of Modified RNAs: Recent Developments (Minireview).”

¹² Jora et al., “Differentiating Positional Isomers of Nucleoside Modifications by Higher-Energy Collisional Dissociation Mass Spectrometry (HCD MS).”

EXPLORING ALTERNATIVE MASS SPECTROMETRIC METHODS
FOR EPITRANSCRIPTOMIC ANALYSIS

by

Hongzhou Wang

A Dissertation
Submitted to
the Faculty of The Graduate School at
The University of North Carolina at Greensboro
in Partial Fulfillment
of the Requirements for the Degree
Doctor of Philosophy

Greensboro

2022

Approved by

Dr. Norman H.L. Chiu
Committee Chair

APPROVAL PAGE

This dissertation written by Hongzhou Wang has been approved by the following committee of the Faculty of The Graduate School at The University of North Carolina at Greensboro.

Committee Chair

Dr. Norman H.L. Chiu

Committee Members

Dr. Ethan Will Taylor

Dr. Nicholas Oberlies

Dr. Qibin Zhang

October 19, 2019

Date of Acceptance by Committee

October 19, 2022

Date of Final Oral Examination

TABLE OF CONTENTS

CHAPTER I: INTRODUCTION.....	1
Epitranscriptomic analysis	1
RNA methylation.....	2
Methodologies for RNA modification analysis.	3
Nanopore Sequencing	4
Liquid Chromatography-Mass Spectrometry (LC-MS) analysis of ribonucleosides.....	5
Disease Model	6
CHAPTER II: APPLICATION OF LC-MS EPITRANSCRIPTOMIC ANALYSIS	9
Introduction	9
Materials and methods	10
Results and Discussion	14
Conclusion	23
Limitation.....	23
CHAPTER III: SIZE REDUCTION ION MOBILITY (SRI) MASS SPECTROMETRY	25
Introduction.....	25
Materials and methods	27
Results and discussion	28
Conclusion	40
CHAPTER IV: FLOW INJECTION ANALYSIS (FIA).....	42
Introduction.....	42
Materials and methods	44
Results and discussion	46
Conclusion	59
REFERENCES	61

CHAPTER I: INTRODUCTION

Epitranscriptomic analysis

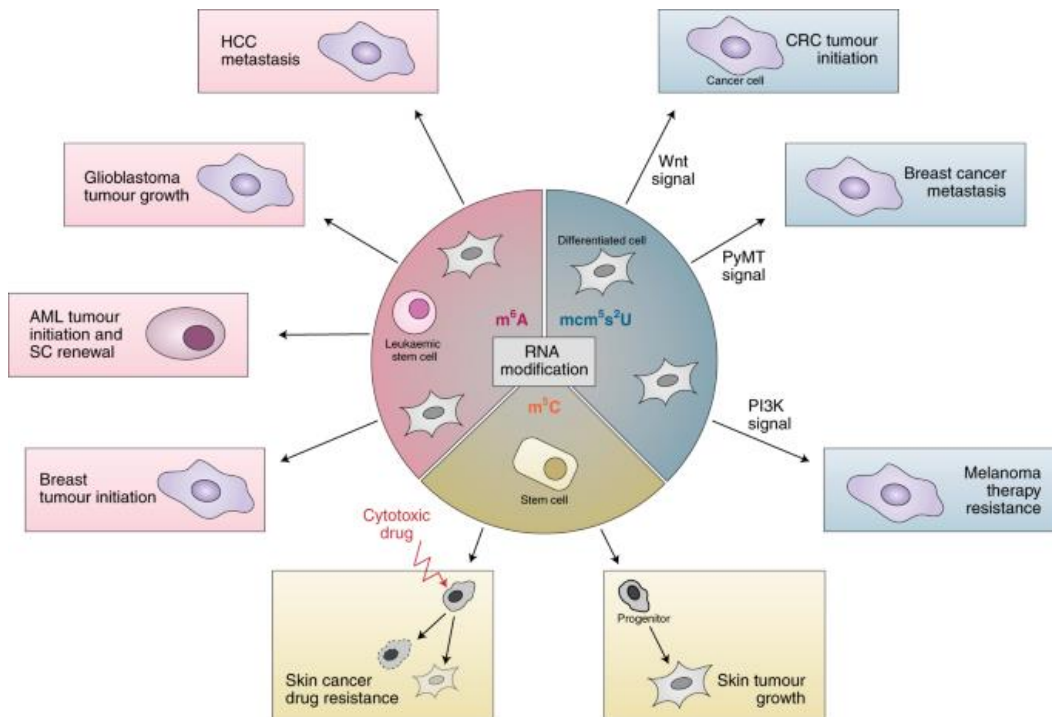
Epitranscriptomic analysis also refer as RNA modification which is currently being use for many science research areas, for example, the modification of RNA molecule could be use as bio markers to monitor the status of organism or cells. Another board domain which scientists apply epitranscriptomic analysis to is mediated regulation of gene expression.¹³ By combine RNA modification identification with sequencing technologies, new ideas in RNA biology could be inspired. Last but not at least, RNA modifications have been shown to play a pivotal role in how the gene responds to environmental impacts and in the development of disease.¹⁴ In other words, epigenetic modification of RNA in response to changes in the surrounding environment can impact a variety of biological processes.¹⁵ Therefore, more and more medicinal researcher starts diverting attention to using RNA modification study diseases especially cancer. No matter for the early diagnosis of cancer or tumor growth monitoring, and the therapy resistance study, epitranscriptomic analysis show great potential.

¹³ Li, Xiong, and Yi, "Epitranscriptome Sequencing Technologies: Decoding RNA Modifications."

¹⁴ Livneh et al., "The m⁶A Epitranscriptome: Transcriptome Plasticity in Brain Development and Function."

¹⁵ Silantjev et al., "Current and Future Trends on Diagnosis and Prognosis of Glioblastoma: From Molecular Biology to Proteomics."

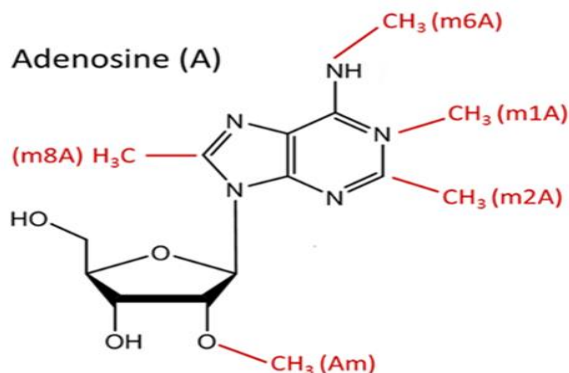
Figure 1. The use of epitranscriptomic analysis in cancer studies.



RNA methylation

Among all kinds of RNA modifications, methylation is the most common and valuable study object. It occurs in different RNAs including tRNA, rRNA, mRNA, tmRNA, snRNA, snoRNA, miRNA, and viral RNA, which epigenetically impact numerous biological processes. For example, ribonucleoside adenosine could have a methyl group attached to 4 different locations of the base, and one possibility for the sugar ring. When methylation happens, the hydrophobicity of the RNA molecule would be affected, and it would cause the stability of Watson-Crick base pairs to also change. In other words, the folding of the RNA chain would also be affected. Therefore, methylation is not only affected on a single ribonucleoside molecule, but the physical properties of different RNA modifications would affect the function of the RNA chains.

Figure 2. The examples of RNA methylation.



Methodologies for RNA modification analysis.

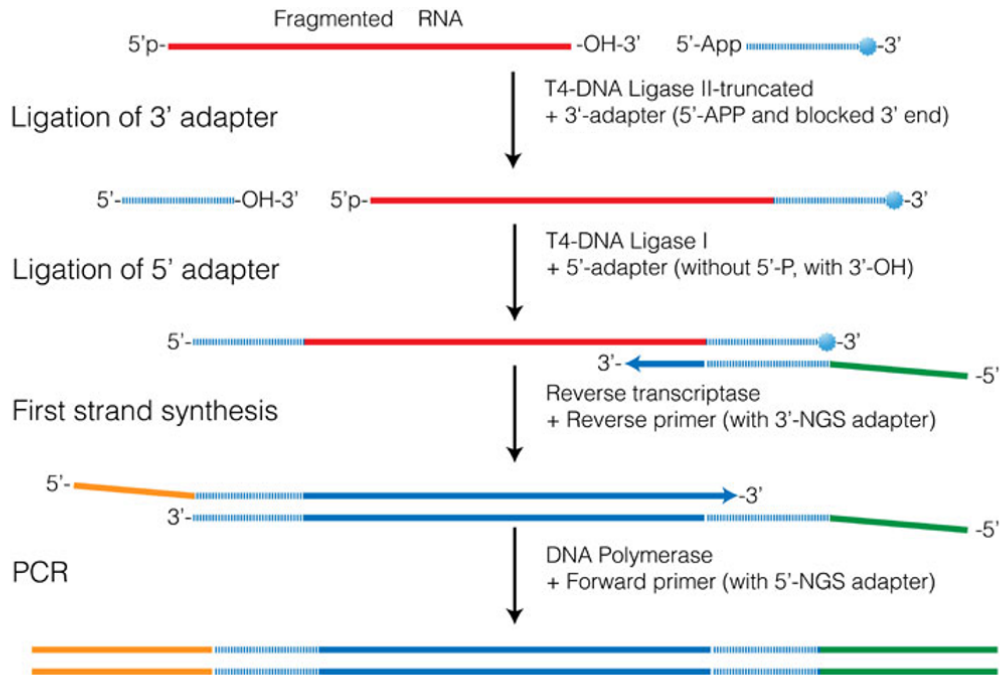
Next Generation Sequencing

The current approach for carrying out epitranscriptomic analysis can be divided into several categories. Firstly, the next generation sequencing (NGS) and other sequencing-based methods have the advantages of providing the exact location of RNA modifications while being a quantitative analysis.^{16,17} However, in general, sequencing methods do not generate the detection signals directly from the modified ribonucleotides, thus sequencing methods are prone to have some errors. In many cases, the rate of errors is relatively low and acceptable. The major drawback of sequencing methods is the incapability to detect all the known RNA modifications in a single experiment.

¹⁶ Schwartz and Motorin, "Next-Generation Sequencing Technologies for Detection of Modified Nucleotides in RNAs."

¹⁷ Li, Xiong, and Yi, "Epitranscriptome Sequencing Technologies: Decoding RNA Modifications."

Figure 3. General approach of sequencing methods.

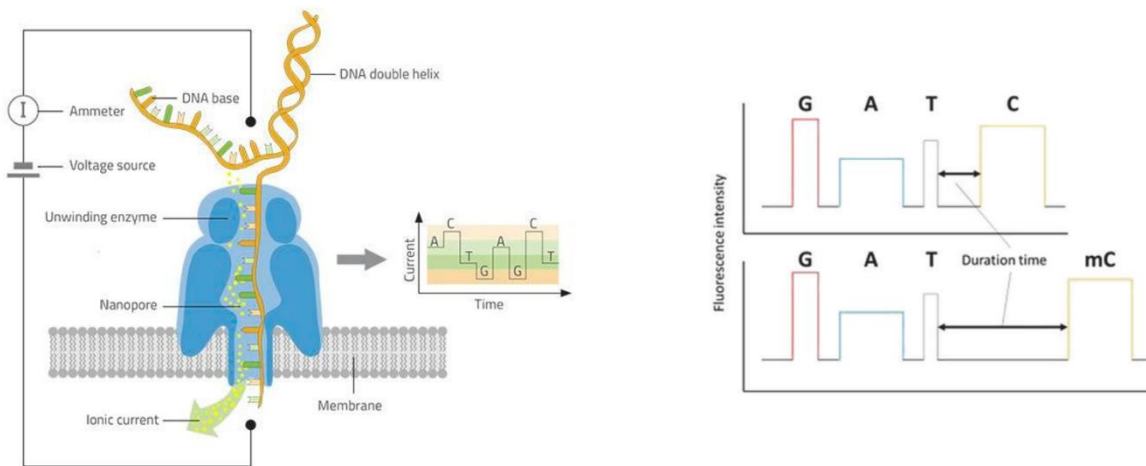


Nanopore Sequencing

The same drawback applies with the probe-based methods. An alternative approach is a technology that measures the variation of current going across a nanopore when a strand of nucleic acid is passing through the nanopore.¹⁸ In principle, the nanopore technology can perform the RNA sequencing at relative high speed. However, its applicability for the detection of RNA modifications is not fully demonstrated yet.

¹⁸ Konno, Taniguchi, and Ishii, "Significant Epitranscriptomes in Heterogeneous Cancer."

Figure 4. General approach of nanopore methods



Liquid Chromatography-Mass Spectrometry (LC-MS) analysis of ribonucleosides

Therefore, until a more suitable method will become available for analyzing the epitranscriptome, the conventional approach of using liquid chromatography mass spectrometry (LC-MS) method to analyze the digested ribonucleosides remains as the most comprehensive approach for profiling all the RNA modifications in a specific epitranscriptome.

Figure 5. Workflow of LC-MS methods.

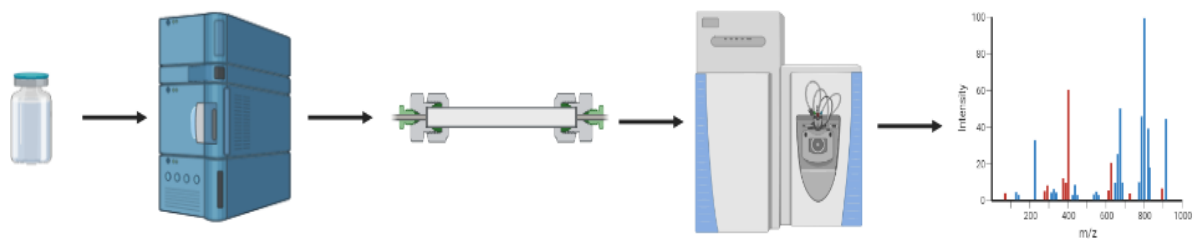
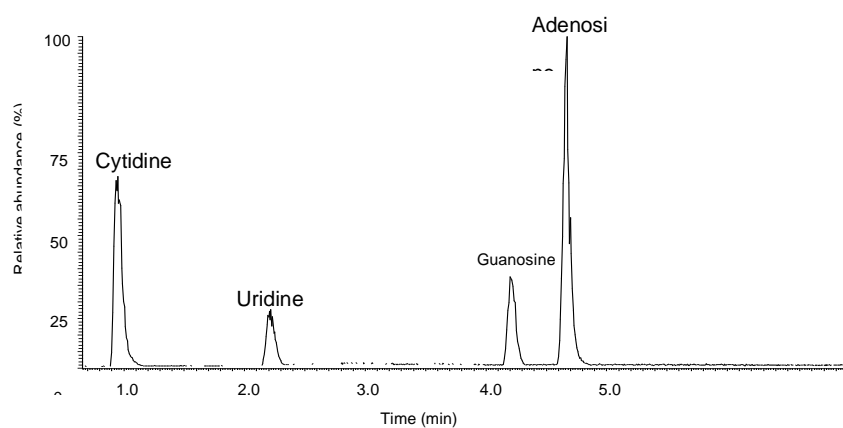


Figure 6. LC-MS ion chromatogram of canonical ribonucleosides mixture.



Disease Model

Glioblastoma (GBM) is the most common primary brain neoplasm. (Current trends in the) Average life expectancy of patients only about 15 months under standard of care treatment. (surgery, radiotherapy, and administration of temozolomide (TMZ) And the 5-year survival rate of GBM is only 5.8%. One of the reason this cancer has such high death rate is lacking

biomarkers for both diagnosis and resistance study. Therefore, GBM is an idea model which can be applied to studying epitranscriptomes.

Table 1. Modifications identified in GBM epitranscriptomic profile.

RNS	RT (± 0.1 min)	Formula	m/z	Accuracy (ppm)	Precision (% RSD)	Fragment Ions
Y	1.0	C ₉ H ₁₂ O ₆ N ₂	245.0771	1.050	0.6	209.0557,179.0451,155.0452
D	0.9	C ₉ H ₁₄ O ₆ N ₂	247.0928	1.527	5.7	115.0506,97.0289
m1acp3Y	1.9	C ₁₄ O ₈ N ₃ H ₂₁	360.1403	0.330	6.0	360.1405,324.1192,294.1081,270.1086,223.0715, 228.4908
m3C	1.3	C ₁₀ O ₅ N ₃ H ₁₅	258.1086	0.747	2.7	126.0664,109.0401,95.0246,82.0294,56.9657
m1A	1.6	C ₁₁ O ₄ N ₅ H ₁₅	282.1199	0.778	0.5	282.1197,150.0775,133.0510,109.0513
m5C	1.7	C ₁₀ O ₅ N ₃ H ₁₅	258.1087	1.096	0.2	126.0661,109.0398,83.0609,56.0503
acp3U	1.7	C ₁₃ O ₈ N ₃ H ₁₉	346.1248	1.008	0.2	346.1246,214.0823,197.0561,168.0768,96.0085,56.0504
ncm5U	1.9	C ₁₁ O ₇ N ₃ H ₁₅	302.0988	1.42	6.5	170.0565
m7G	2.7	C ₁₁ O ₅ N ₅ H ₁₇	298.1149	0.956	3.3	298.1147,166.0724,149.0458,124.0508,69.0455
Cm	2.9	C ₁₀ O ₅ N ₃ H ₁₅	258.1087	0.980	0.4	112.0509,95.0245,69.0455
m1Y	3.1	C ₁₀ O ₆ N ₂ H ₁₄	259.0927	1.07	0.8	169.0608,179.0452,227.0650,209.0551
I	3.9	C ₁₀ O ₅ N ₄ H ₁₂	269.0883	0.758	3.9	137.0459,119.0355,110.0353,56.9656
m5U	4.1	C ₁₀ O ₆ N ₂ H ₁₄	259.0927	0.723	2.5	127.0504,110.0241,84.9603,56.9656
Um	4.8	C ₁₀ O ₆ N ₂ H ₁₄	259.0928	1.341	0.1	113.0349,147.0652,96.0085,70.0295
m3U	4.9	C ₁₀ O ₆ N ₂ H ₁₄	259.0928	1.148	0.8	127.0504,96.0085,84.9604,56.9656
m1G	5.4	C ₆ H ₈ ON ₅ *	166.0724	0.563	3.2	166.0724
Gm	5.4	C ₅ H ₆ ON ₅ *	152.0568	0.55	1.3	152.0568
m1I	5.4	C ₁₁ O ₅ N ₄ H ₁₄	283.1039	0.791	0.4	151.0616,110.0352,82.0406,56.9656
mcm5U	5.6	C ₁₂ O ₈ N ₂ H ₁₆	317.0984	1.102	7.0	185.0561
m2G	5.6	C ₁₁ O ₅ N ₅ H ₁₅	298.1148	0.788	0.9	298.1144,166.0725,149.0458,135.0302(loss of CH5N),128.0456,110.0353
ac4c	5.7	C ₁₁ O ₆ N ₃ H ₁₅	286.1035	0.588	0.8	154.0612,112.0509,95.0246,69.0455
Am	5.7	C ₁₁ O ₄ N ₅ H ₁₅	282.1199	0.814	1.0	282.1198,136.0619,119.0356,92.0250,67.0299
m2,2,7G	5.8	C ₁₃ O ₅ N ₅ H ₂₁	326.1462	0.935	0.5	194.1038,167.0565,124.0508
m5Um	6.2	C ₁₁ O ₆ N ₂ H ₁₆	273.1083	0.649	1.2	127.0504,110.0242
m6A	6.4	C ₁₁ O ₄ N ₅ H ₁₅	282.1199	0.991	0.7	282.1198,150.0775,123.0668,133.0508,108.0435,94.0406
m2,2G	6.5	C ₁₂ O ₅ N ₅ H ₁₇	312.1304	0.560	2.4	312.1299,180.0880
mcm5s2U	7.1	C ₁₂ O ₇ N ₂ H ₁₆ S	333.0754	0.877	1.9	201.0329,169.0067,141.0116
m6Am	7.4	C ₁₂ O ₄ N ₅ H ₁₇	296.1356	0.842	0.2	296.1356,150.0775,108.0434,94.040
m6,6A	8.1	C ₁₂ O ₄ N ₅ H ₁₇	296.1356	0.91	0.1	296.1354,164.0932,120.0433 (loss of C2H6N)
t6A	8.2	C ₁₅ O ₈ N ₆ H ₂₀	413.1421	1.239	0.2	281.0994,162.0410,136.0618,119.0355
m6t6A	9.0	C ₁₆ O ₈ N ₆ H ₂₂	427.1578	1.456	1.0	295.1149,150.0776,123.0669,108.0435
ms2t6A	9.4	C ₁₆ O ₈ N ₆ H ₂₂ S	459.1298	1.353	2.1	327.0869,208.0288,134.0463
i6A	10.7	C ₁₅ O ₄ N ₅ H ₂₁	336.1668	0.623	7.7	336.1667,204.1245,136.0618,148.0618

Epitranscriptomic analysis as a new field of study was developed to help study GBM, especially the exploring the resistance of chemotherapy. The dysregulation of specific RNA modifications and their associated enzymes in disease states, suggests their importance. However, there are no reports to date regarding the association of specific profiles of RNA modifications in cancer or GBM. Our research group already created a unique LCMS method to achieve 81% coverage of the epitranscriptome of glioblastoma with 96% accuracy is detailed and

validated. The modulation of the GBM epitranscriptome to one of temozolomide (TMZ) resistance is delineated in vitro and in vivo. Also, the upregulation of 5-methylcytidine (m5C), N6-threonylcarbamoyladenosine (t6A), and N6-methyl-N6-threonylcarbamoyladenosine (m6t6A), are identified as target biomarkers in GBM resistant to TMZ. Knockdown of the specific writer gene for the RNA modification m6t6A, tRNA methyltransferase O (TRMO), shows promise for desensitization to TMZ treatment in preclinical GBM models.

CHAPTER II: APPLICATION OF LC-MS EPITRANSCRIPTOMIC ANALYSIS

Introduction

Collectively, all the RNA molecules in a specific group of cells are referred as a epitranscriptome. In order to achieve some of the RNA functionalities, the RNA structure can be altered by more than 170 different RNA modifications.^{19,20} The presence of a RNA modification is the result of an enzymatic reaction of its corresponding writer enzyme. In contrast, RNA modification can be removed by a different enzyme called eraser. To recognize the importance of RNA modifications to the RNA structures and functions, the term of epitranscriptome was coined by Mason and his associates.²¹ There are reports indicating specific epitranscriptomes are linked to a variety of health-related issues.^{22,23} With the interests in studying epitranscriptomes, a number of methods for analyzing RNA modifications have been developed.^{24,25} Among those methods, mass spectrometric (MS) based method is the only universal approach for detecting different RNA modifications.

Lactobacillus species are common constituents of gastrointestinal tracts,²⁶ and have been used as probiotics.²⁷ Prebiotics are defined as substrates that are utilized by microorganisms

¹⁹ Yanas and Liu, "RNA Modifications and the Link to Human Disease."

²⁰ Jordan Ontiveros, Stoute, and Liu, "The Chemical Diversity of RNA Modifications."

²¹ Saletore et al., "The Birth of the Epitranscriptome: Deciphering the Function of RNA Modifications."

²² Yanas and Liu, "RNA Modifications and the Link to Human Disease."

²³ Barbieri and Kouzarides, "Role of RNA Modifications in Cancer."

²⁴ Chen, Yuan, and Feng, "Analytical Methods for Deciphering RNA Modifications."

²⁵ Chen, Yuan, and Feng; Lauman and Garcia, "Unraveling the RNA Modification Code with Mass Spectrometry."

²⁶ Heeney, Gareau, and Marco, "Intestinal Lactobacillus in Health and Disease, a Driver or Just along for the Ride?"

²⁷ Lebeer et al., "Identification of Probiotic Effector Molecules: Present State and Future Perspectives."

conferring health benefits.²⁸ One of the most commonly used prebiotics is inulin.²⁹ Since inulin cannot be metabolized by human digestive enzymes, the digestion of inulin relies on gut microbes.³⁰ In this chapter, we use the MS method to profile the *L. agilis* epitranscriptome, and subsequently determine whether the *L. agilis* epitranscriptome is involved in the adaptation to inulin.

Materials and methods

E. coli alkaline phosphatase, Benzoylase nuclease and bovine serum albumin (BSA) were purchased from Sigma-Aldrich (St. Louis, MO, USA). The venom exonuclease phosphodiesterase I was purchased from Worthington Biochemical Corp. (Lakewood, NJ, USA). All other solvents were purchased from Thermo Fisher Scientific (Waltham, MA).

Culturing of L. agilis

A *Lactobacillus agilis* strain named YZ050 was previously isolated from dairy cow fecal samples in our lab and showed the capability to ferment inulin.³¹ The stock was streaked on MRS plates. After 24 hours, a MRS broth was inoculated and cultivated at 37 °C under anaerobic conditions. The overnight culture (1%) was inoculated into basal MRS media supplemented with 1% inulin or 1% glucose. After ~5 hrs, samples were taken for RNA extraction at mid-log phase.

²⁸ Swanson et al., “The International Scientific Association for Probiotics and Prebiotics (ISAPP) Consensus Statement on the Definition and Scope of Synbiotics.”

²⁹ “Inulin - a Versatile Polysaccharide: Use as Food Chemical and Pharmaceutical Agent | Journal of Excipients and Food Chemicals.”

³⁰ Le Bastard et al., “The Effects of Inulin on Gut Microbial Composition: A Systematic Review of Evidence from Human Studies.”

³¹ Zhu et al., “Inulin Fermentation by Lactobacilli and Bifidobacteria from Dairy Calves.”

Extraction of RNA

Cells were pelleted and resuspended in 1 mL RNAprotect Bacteria Reagent (Qiagen Inc, Valencia). The cells were washed twice with 1X PBS and pre-lysed with 250 μ L 50 g/L lysozyme and 120 μ L 1000 units/mL mutanolysin. Total RNA was extracted using the RNeasy mini kit (Qiagen Inc, Valencia). Total RNA samples were DNase-treated twice, and the absence of genomic DNA was confirmed by PCR.

Depletion of ribosomal RNA (rRNA)

Ribosomal RNA was removed using the RiboMinus Transcriptome Isolation Kit, (Thermo Fisher, Waltham, MA). The integrity of RNA was assayed using the 2100 Bioanalyzer (Agilent Technologies, Santa Clara, CA).

Digestion of rRNA-depleted RNA

Each RNA sample was digested in an enzymatic reaction of 25 μ L at 37 °C for 3 hours, which contained 5 μ g rRNA-depleted RNA, 0.05 units phosphodiesterase I, 0.5 units alkaline phosphatase, 5 units benzonase, 50 mM Tris-HCl (pH 8.0), 1 mM MgCl₂ and 0.1 mg/mL BSA.³² After removing the enzymes with 3K MWCO spin filter at 14,000g for 15 mins (Pall Corporation, Port Washington, NY), the digested RNA sample was diluted in deionized water to 50 ng/ μ L.

UPLC-MS/MS analysis of digested RNA

An Acquity ultra-high performance liquid chromatography (UPLC) system (Waters Corporation, Milford, MA) which was equipped with an Acquity HSS T3 column (2.1 x 50 mm, 1.8 μ m) and a HSS T3 VanGuard pre-column (2.1 x 5 mm, 1.8 μ m) at 30 °C was used. After

³² Su et al., "Quantitative Analysis of Ribonucleoside Modifications in tRNA by HPLC-Coupled Mass Spectrometry."

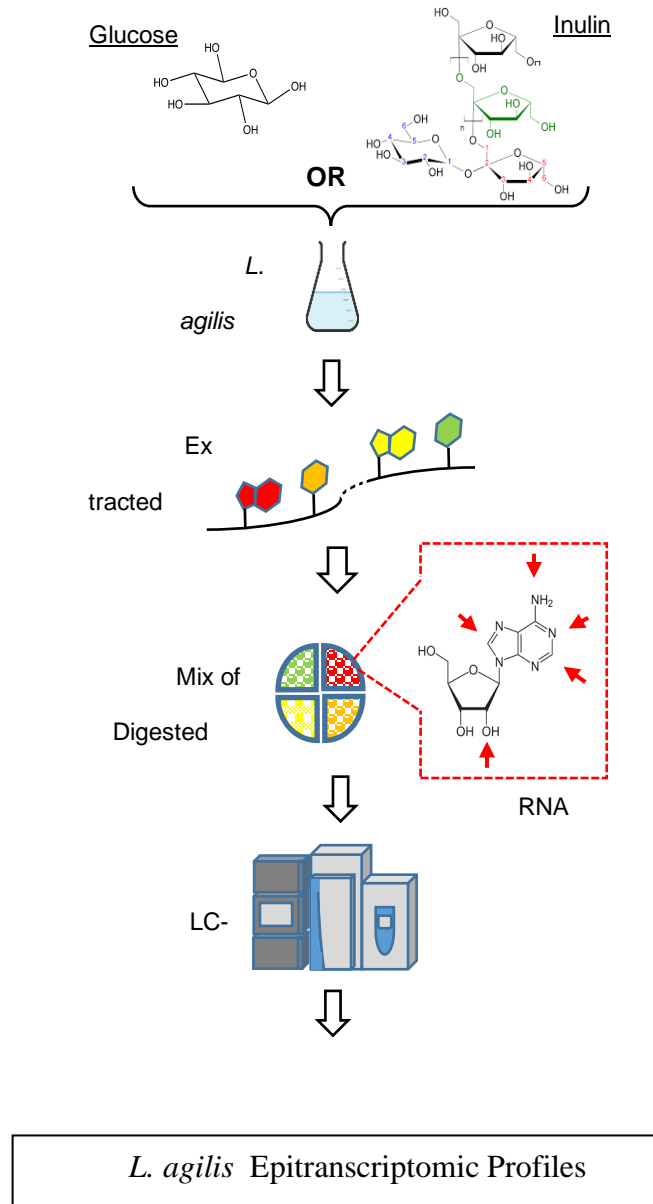
injecting 10 μ L of sample, the elution was carried out with a binary solvent system, in which solvent A contained water and 0.01 % (v/v) formic acid, and solvent B contained 50 % acetonitrile and 0.01 % (v/v) formic acid at a flowrate of 0.4 mL/min. The gradient elution profile initiated at 100:0 (A:B) from 0.0 – 0.5 min., ramping to 70:30 from 0.5 – 9 mins, followed by 50:50 from 9 – 10 mins, and ended with 0:100 from 10 – 17 mins. Randomized injections were used. The negative control was prepared without any RNA sample.

Tandem mass spectrometry (MS/MS) was performed on a Q Exactive Plus (Thermo Fisher Scientific, Waltham, MA) in the positive mode with ESI at 425 °C and 3.5 kV. Sheath and auxiliary gas flow were at 50 and 13 arbitrary units, respectively. Data was acquired with an inclusion list of calculated m/z of all known RNA modifications. The mass calibration was performed using a canonical ribonucleoside standard mixture (3ng/ μ L). Data analysis was carried out with Xcalibur (Thermo Fisher Scientific, Waltham, MA) restricting the precursor ion to ≤ 5 ppm accuracy and its retention time to ≤ 0.1 min.

RNA sequencing (RNAseq)

Each library was generated from 20 ng rRNA-depleted RNA sample using the Kapa Hyper Stranded RNA-seq kit (KapaBiosystems, Cape Town, South Africa). The consistency of the libraries was verified by 2100 Bioanalyzer. The libraries were quantified by fluorometry and sequenced on a NextSeq 500 (Illumina, San Diego, CA) with paired-end 75p reads. The sequence files were processed using the CLC-Bio Genomics Workbench (CLC Bio, Denmark).

Figure 7. Design and workflow in the protocol that was used to establish and compare the *L. agilis* epitranscriptomic profiles associated with the use of either glucose or inulin in the culturing medium. The red arrows represent the possible location of RNA modifications.



Results and Discussion

The notions for epitranscriptome to be a standalone investigation include a single RNA modification can potentially alter the RNA interactions.³³ There are also evidence showing unique epitranscriptomes are associated with specific phenotypes.³⁴ Together with the discovery of various writer genes for RNA modifications, a specific epitranscriptome is considered to represent a set of specific codes for regulating cellular activities.³⁵ Our initial efforts focused on establishing the profile of *L. agilis* epitranscriptome. Among various types of RNA, ribosomal RNA (rRNA) makes up ~80 % of total RNA.³⁶ To better witness bacterial gene expression, rRNA is often depleted from the RNA samples prior to sequencing. Equivalently, rRNA was also removed in our protocol, otherwise would reduce the detectability of RNA modifications that are unique in other types of RNA. The removal of rRNA can also enhance our ability to detect any variations on the levels of some specific RNA modifications.

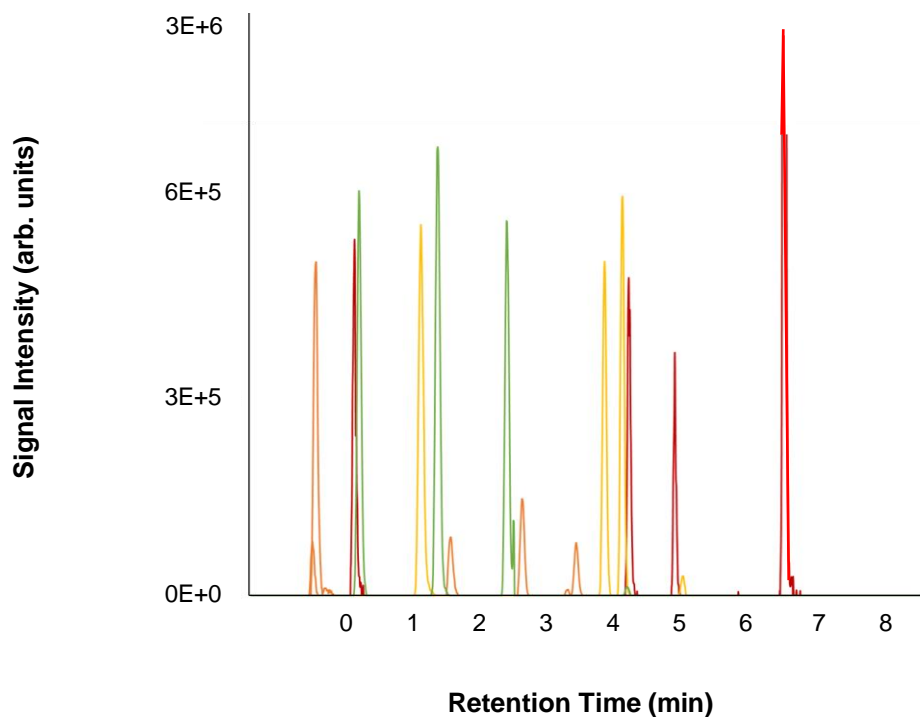
³³ Lewis, Pan, and Kalsotra, “RNA Modifications and Structures Cooperate to Guide RNA-Protein Interactions.”

³⁴ Ranjan and Leidel, “The Epitranscriptome in Translation Regulation: MRNA and TRNA Modifications as the Two Sides of the Same Coin?”

³⁵ Kadumuri and Janga, “Epitranscriptomic Code and Its Alterations in Human Disease.”

³⁶ Rosenow et al., “Prokaryotic RNA Preparation Methods Useful for High Density Array Analysis: Comparison of Two Approaches.”

Figure 8. Overlay of extracted ion chromatograms obtained from the analysis of glucose-associated *L. agilis* RNA sample in the absence of rRNA and digested with the protocol as stated in the methods section. Red = modified adenosine; Orange = modified uridine; Yellow = modified guanosine; Green = modified cytidine.



The results obtained from analyzing all the detectable ribonucleosides in a *L. agilis* sample with a signal-to-noise ratio of ≥ 2 are shown in Table 1. To ensure the low abundant RNA modifications could be detected, the chromatography and signal intensity in the UPLC-MS/MS analysis were optimized. As low as 0.4 pg/uL of each canonical ribonucleoside standard were detected in our calibration experiments. For identifying the RNA modification, both MS and MS/MS data must match with the expected values with <5 ppm error. For the MS/MS measurements, at least two fragment ions were identifiable. The profiling was repeated four times with different samples, and the same profile of RNA modifications were detected each time. To

the best of our knowledge, this is the first time the profile of *L. agilis* epitranscriptome (minus the rRNA modifications) is reported.

Table 2. LC-MS data obtained from the glucose-associated *L. agilis* transcriptome in the absence of rRNA. * ± 0.01 min. **Mass of protonated precursor ion. *Reference to the monoisotopic mass of protonated precursor ion.**

Ribonucleoside Detected and Its Short Name	Retention Time* (min)	Measured Mass** (Da)	Mass Accuracy*** (ppm)
Cytidine, C	0.90	244.0935	0.7
Dihydrouridine, D	0.94	247.0933	3.3
Pseudouridine, Y	0.98	245.0775	3.0
1-methyladenosine, m1A	1.55	282.1205	3.1
5-methylcytidine, m5C	1.63	258.1093	3.2
Uridine, U	2.00	245.0776	3.3
7-methylguanosine, m7G	2.54	298.1155	3.1
2'-O-methylcytidine, Cm	2.79	258.1093	3.2
2'-O-methylpseudouridine, Ym	2.99	259.0934	3.5
Guanosine, G	3.99	284.0997	2.8
5-methyluridine, m5U	4.06	259.0933	3.2
Adenosine, A	4.45	268.1048	2.8
3-methyluridine, m3U	4.86	259.0933	3.1
1-methylguanosine, m1G	5.27	298.1155	3.2
2'-O-methylguanosine, Gm	5.27	298.1155	3.2
N2-methylguanosine, m2G	5.53	298.1155	3.1
N4-acetylcytidine, ac4C	5.61	286.1034	0.2
2'-O-methyladenosine, Am	5.64	282.1204	2.8
N6-methyladenosine, m6A	6.31	282.1206	3.2
N6,N6-dimethyladenosine, m6,6A	7.93	296.1354	0.2
N6-threonylcarbamoyladenosine, t6A	8.04	413.1417	0.8

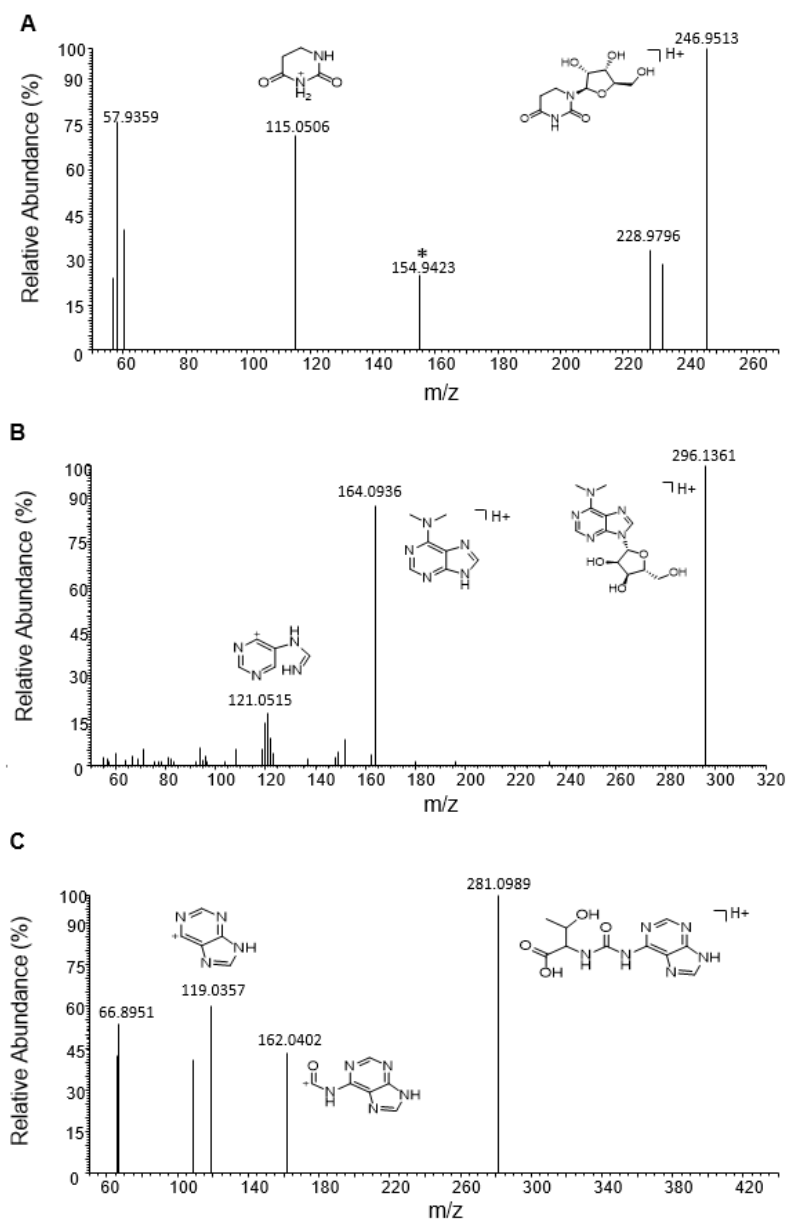
Before determining whether there were any variations on the level of each specific RNA modification, the use of our method to perform accurate quantitative analysis was evaluated. Specifically, a calibration experiment with a series of standard dilutions was performed. The

results indicate the linearity and the dynamic range of the four canonical ribonucleoside standards match or exceed the earlier reports with < 6 % relative standard deviation (n = 3).^{37,38}

³⁷ Basanta-Sanchez et al., “Attomole Quantification and Global Profile of RNA Modifications: Epitranscriptome of Human Neural Stem Cells.”

³⁸ He et al., “Simultaneous Quantification of Nucleosides and Nucleotides from Biological Samples.”

Figure 9. MS/MS spectrum of selected modified ribonucleotide ions that were down-regulated in inulin-associated *L. agilis* epitranscriptome and were unavailable in the public databases of mass spectra. (A) dihydrouridine, (B) *N*6,*N*6-dimethyladenosine and (C) *N*6-threonyl-carbamoyladenosine. * Fragment ion that corresponds to the co-eluted pseudouridine.

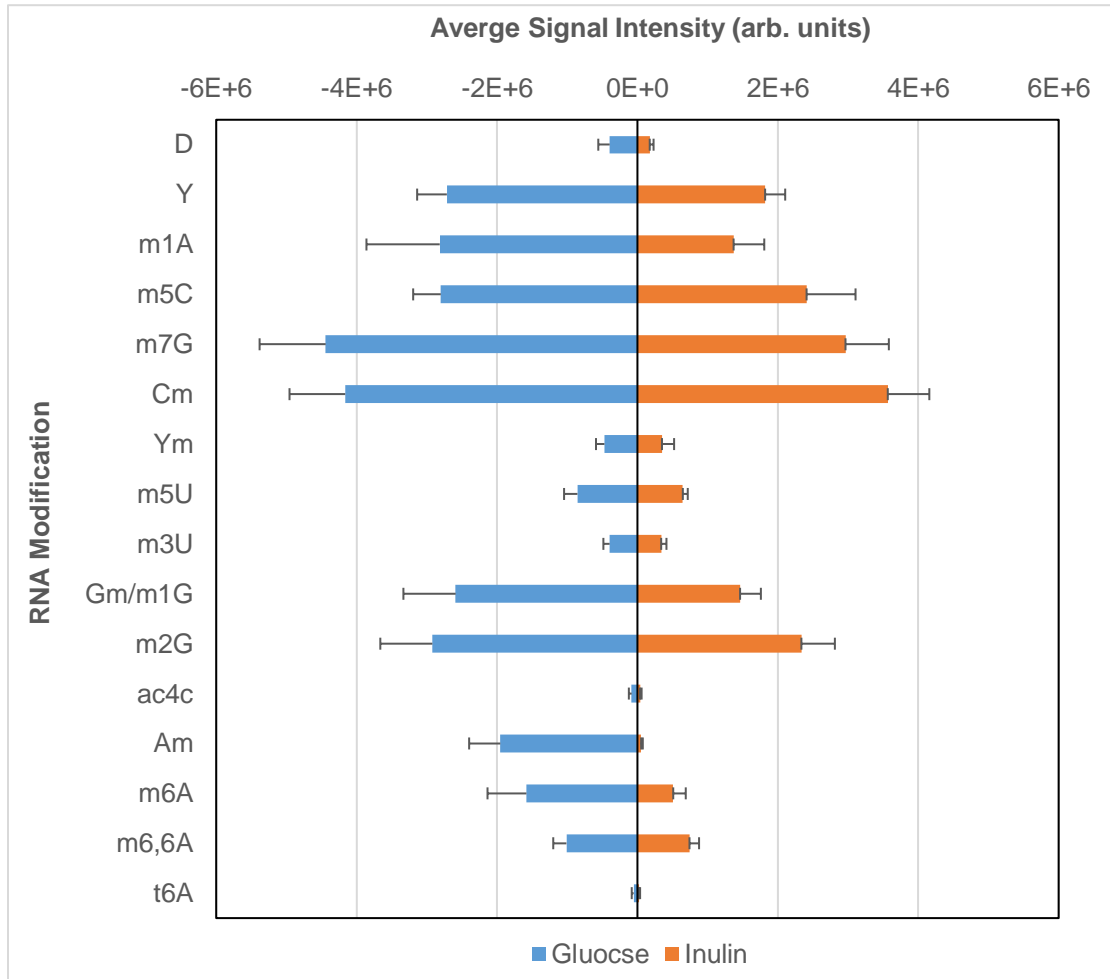


Glucose-Associated vs. Inulin-Associated L. agilis Epitranscriptome

The reproducibility of the *L. agilis* epitranscriptomic profile prompted us to investigate whether the *L. agilis* epitranscriptome would become different when different prebiotic was used. As shown in Fig 1, the RNA modifications found in the inulin-associated *L. agilis* epitranscriptome match with those listed in Table 1. However, there is an obvious downward trend when the cells were cultivated in inulin instead of glucose. However, the fold change of each individual RNA modification was not uniform, with 2'-O-methyladenosine (Am) to be down regulated most. From the chemical point of view, the 2'-O-methylation can disrupt the interactions between 2'-O-methylated RNA and RNase, thus protecting the 2'-O-methylated RNA from the RNase activity.³⁹ Therefore, when the level of Am was lowered in the inulin-associated *L. agilis* transcriptome, it would allow the *L. agilis* transcriptome to be turned over more effectively via the RNase digestion, which could be one way to rearrange the composition of the *L. agilis* transcriptome.

³⁹ Egli et al., "Probing the Influence of Stereoelectronic Effects on the Biophysical Properties of Oligonucleotides: Comprehensive Analysis of the RNA Affinity, Nuclease Resistance, and Crystal Structure of Ten 2'-O-Ribonucleic Acid Modifications."

Figure 10. Mirrored histogram of glucose- or inulin-associated *L. agilis* epitranscriptomic profiles obtained from rRNA-depleted total RNA. *The signals of m6,6A were scaled down 10-folds. Each error bar represents one standard deviation with $n \leq 12$.

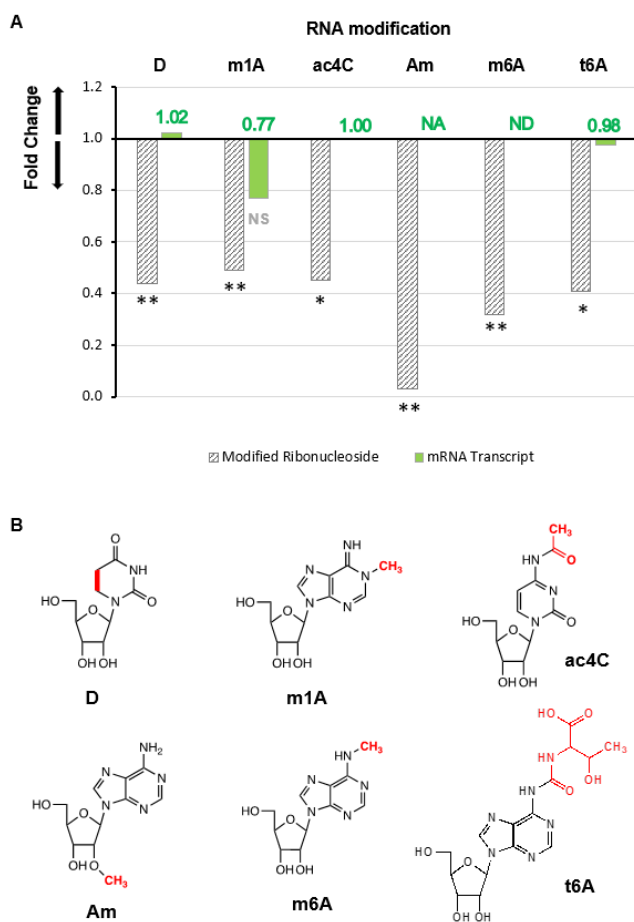


Among all seventeen RNA modifications witnessed in the *L. agilis* epitranscriptome, six of them were down regulated more than the average fold change of 0.65. The top six down-regulated RNA modifications include dihydrouridine (D), 1-methyladenosine (m1A), 4-acetylcytidine (ac4C), 2'-O-methyladenosine (Am), N6-methyladenosine (m6A) and N6-

threonylcarbamoyl-adenosine (t6A). In the case of D modification, the hydrogenation at the 5 and 6 positions of uridine eliminate the only π bonding, thus weakening the effects of base stacking.⁴⁰

Whereas, the modifications of m1A, ac4C, m6A and t6A would interfere with the Watson-Crick base pairing. Therefore, the down regulation of those modifications could potentially change some of the RNA folding and/or annealing.

Figure 11. Fold change on the levels of modified ribonucleoside and their molecular structure

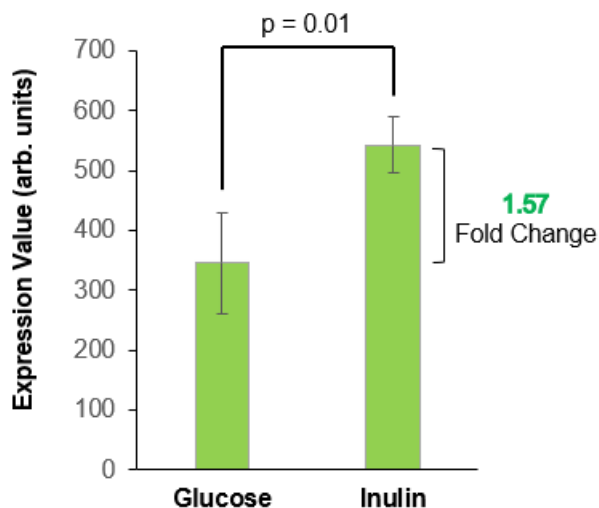


⁴⁰ Dalluge et al., "Posttranscriptional Modification of tRNA in Psychrophilic Bacteria."

(A) Fold changes on the levels of detectable modified ribonucleoside or mRNA transcript that corresponds to the writer of the top six down-regulated RNA modifications that resulted from switching glucose to inulin. The numerical numbers show the exact fold changes in the expression of corresponding writer gene. NA = Gene identity not available; ND = Gene not detected; NS = Not significant; * $p < 0.05$; ** $p < 0.01$. (B) Molecular structure of the top six down-regulated RNA modifications, with the group corresponding to the modification highlighted in red.

Since no information on the eraser for the top six down-regulated RNA modifications could be found, our investigation on the down regulation of *L. agilis* epitranscriptome focused only on the writers. The results from comparing our gene expression data find no difference on the levels of writer for t6A, D, m1A and ac4C (Fig 11A). The writer gene for Am in *L. agilis* is not known. Also, no transcript corresponding to the m6A writer could be detected. Theoretically, an alternative way to remove RNA modifications could simply rely on the non-specific digestion of modified RNA. For this reason, the expression levels of all detectable ribonuclease in *L. agilis* were compared, which included RNase 3, RNase HI, RNase HII, J1, RNase R, RNase Y and RNase Z. In the case of RNase J1, a significant increase on its expression level was found among the inulin samples (Fig. 11B). For all the other ribonucleases, no difference was detected. Hence, the higher expression level of RNase J1 could be the cause for the down regulation of the inulin-associated *L. agilis* epitranscriptome.

Figure 12. Difference in expressing the RNase J1 gene in *L. agilis*. Error bars represent one standard deviation (n = 4).



Conclusion

When *L. agilis* cells were cultivated with glucose being the sole source of energy, the *L. agilis* epitranscriptome consists of seventeen different RNA modifications at variable abundance. There was a downward trend across the entire *L. agilis* epitranscriptome when the cells were exposed to inulin instead of glucose. To the best of our knowledge, this marks the first report on a system-wide variation of a bacterial epitranscriptome that resulted from adapting to an alternative source of energy. By comparing the gene expression data, the inulin-associated *L. agilis* epitranscriptome could be down regulated by the RNase J1 activity. Overall, these results further strengthen the association of a unique epitranscriptome to a specific cellular activity.

Limitation

LC-MS is a suitable technique for epitranscriptomic analysis that can be applied to all types of cells. However, it has two aspects that can be improved. Firstly, although the LC column could resolve most of ribonucleosides in the sample of interest, as shown in figure 8, some of the

peaks are not completely resolved from each other. In other words, their co-elution is unavoidable, especially when those co-elution compounds are isomers, it does require additional measurements or data for identifying the isomeric RNA modifications.

Another disadvantage for LC-MS method is the time spending on each sample analysis is relatively long. To separated compounds from a sample mixture, the LC separation usually requires 15 – 30 minutes per sample. In the case of our *L. agilis* study, 25 minutes per sample is required. It is acceptable for an exploratory study, but to apply the LC-MS method to a larger study including clinical study, a high sample throughput method is needed.

CHAPTER III: SIZE REDUCTION ION MOBILITY (SRI) MASS SPECTROMETRY

Introduction

RNA is sub-divided into several types of RNA, such as message RNA, transfer RNA, and microRNA. In terms of the basic RNA structure, it is made up of only four different building blocks, namely, adenosine, uridine, guanosine, and cytidine. The composition and the order of these ribonucleotides, i.e., RNA sequence, define the identity of each RNA molecule. However, in order to achieve some of the RNA functionalities, the molecular structure of RNA can be altered by a whole spectrum of posttranscriptional modifications. It is important to note that RNA modifications are different from RNA editing, which focuses on the changes of RNA sequence, whereas RNA modifications refer mainly to the changes in the molecular structure of ribonucleotides. a group of different isomers are generated. The molecular mass of each isomeric RNA modification is of course identical to each other, but their corresponding physical and chemical properties are slightly different. For instance, two of the isomers of methylated adenosine, namely, 1methyladenosine (m1A) and N6-methyladenosine (m6A), can disrupt their base pairing with uridine, but the extent of disruption is different. Since the proper base pairing between two complementary RNA sequences is crucial to the formation of specific RNA folding or RNA duplexes, it is therefore important to distinguish which of the two isomers are present in the modified RNA molecules.

With the advances in the annotation of genomes, there are growing interests to tackle the analysis of RNA modifications at the transcriptomic level.^{41,42,43,44,45} When using the LC-MS method to accurately identify a specific RNA modification, it requires the accurate mass of the modified ribonucleoside ion and at least one of the corresponding CID (collision-induced dissociation) fragment ion to be detectable. To differentiate the isomeric RNA modifications, it also requires a unique CID fragment ion that corresponds to the isomer of interest to be detectable. This in turn may require more precursor ions to be available for the CID process. For LC-MS analysis, the amount of a specific precursor ions is dependent on a number of factors, which include the sample concentration, the flow rate of the mobile phase, the ionization efficiency of the eluted sample, and the duration of the time window during which the sample is being eluted from the LC column. In addition, the use of an optimal CID energy may require to break off the unique CID fragment ion from the precursor ion. Hence, IM measurements are independent to the MS measurements. From the perspective of sample identification, the IM data can be used to support the MS data and further enhance the accuracy on the sample identification. The Fabris group had published the first chromatographic-free report on using IM-MS to analyze epitranscriptome.⁴⁶ More recently, the Kammerer group had used the same IM-MS method to determine the profile of ribonucleosides that exist in cell culturing medium of

⁴¹ Licht and Jantsch, “Rapid and Dynamic Transcriptome Regulation by RNA Editing and RNA Modifications.”

⁴² Basanta-Sanchez et al., “Attomole Quantification and Global Profile of RNA Modifications: Epitranscriptome of Human Neural Stem Cells.”

⁴³ Nachtergaele and He, “Chemical Modifications in the Life of an mRNA Transcript.”

⁴⁴

⁴⁵ Huber et al., “The Versatile Roles of the tRNA Epitranscriptome during Cellular Responses to Toxic Exposures and Environmental Stress.”

⁴⁶ Rose et al., “Profiling Ribonucleotide Modifications at Full-Transcriptome Level: A Step toward MS-Based Epitranscriptomics,” July 1, 2015.

different cancer cell lines.⁴⁷ In both cases, the reported arrival time distribution (ATD) of each individual isomeric ribonucleoside ion were very close to each other and might exceed the available ion mobility resolution.⁴⁸ In this report, by using the same IM platform, our goals are to explore a way to achieve a more effective IM separation by reducing the size of ions prior to the IM measurements and apply the improvement to enhance the accuracy for identifying specific isomeric RNA modifications.

Materials and methods

Adenosine and N1-methyladenosine (m1A) were obtained from Sigma-Aldrich (St. Louis, MO, USA). N6Methyladenosine (m6A), 3-methylcytidine (m3C), and 5methylcytidine (m5C) were purchased from Carbosynth (Compton, Berkshire, UK). Acetonitrile (ACN), formic acid, and water at the Optima LC/MS grade were purchased from Thermo Fisher Scientific (Hampton, NH, USA). All the stock solution (5 mM) of unmodified and modified ribonucleoside were prepared with deionized water and stored at -20°C . In each experiment, $70\ \mu\text{M}$ of freshly diluted standard solution was prepared with 50% ACN/water and 0.01% formic acid, which resembles the mobile phase being used in our laboratory for the conventional LC-MS/MS analysis of specific epitranscriptomes.

Ion mobility mass spectrometric measurements

All experimental data was acquired using the Waters Synapt G2 high definition mass spectrometer (Waters, Milford, MA, USA), which was equipped with an electrospray (ESI) source. Each sample was delivered by direct infusion at a flow rate of $10\ \mu\text{L}/\text{min}$. The source

⁴⁷ Lagies et al., “Unraveling Altered RNA Metabolism in Pancreatic Cancer Cells by Liquid-Chromatography Coupling to Ion Mobility Mass Spectrometry.”

⁴⁸ Giles, Williams, and Campuzano, “Enhancements in Travelling Wave Ion Mobility Resolution.”

temperature was set at 80 °C, the desolvation temperature at 200 °C, the gas flow rate at the cone was maintained at 50 L/h, and the desolvation gas flow rate at 800 L/h while the other ESI parameters were optimized to attain the highest mass spectrometric signal without any detectable in-source fragmentation. Unless otherwise stated, the traveling wave ion mobility (TWIM) components were operated under the default settings, which included a flow of Argon gas to the trap and transfer cell at 2 mL/min, a flow of helium gas to the helium cell at 180 mL/min, a flow of nitrogen gas to the ion mobility cell at 30 mL/min, the wave height at 30 V, and the wave velocity at 1200 m/s. The time-of-flight (TOF) mass analyzer was operated under the resolution mode, and the negative ion mode was used. After switching to the IM mode, approximately 5 min wait time was given for the pressure within the TWIM components to be stabilized. In each experiment, the signals from each sample were acquired for 30 s. At the end of measuring each standard dilution, the setup for carrying out the direct infusion and the ion source were rinsed out with at least 1 mL of 50% ACN/water at the maximum flow rate (100 μ L/min). All the data acquisition and analysis were carried out with the MassLynx software program (version 4.1) from Waters.

Results and discussion

Enhanced ion mobility (IM) separation of isomeric RNA modifications.

Although the presence of structural isomers is well known, the differentiation of different isomers, including those among RNA modifications, remains as a challenging task. The goal of this investigation is to explore a more effective way to differentiate ribonucleoside ions by using IMS, such that IM data can be used to support the conventional tandem mass spectrometric (MS/MS) data and more accurate identification of isomeric RNA modifications can be accomplished. To enhance the IM separation of ribonucleoside ions, our strategy is to reduce the

size of ribonucleoside ions. The rationale of this concept stems from the fact that there are only four canonical ribonucleotides in RNA molecules, namely, adenosine, uridine, guanosine, and cytidine. Partly due to the simplicity of RNA structure, modified RNAs are normally digested into single ribonucleotides prior to the measurements. The majority of the known RNA modifications involve the addition of a small chemical group. For instance, adenosine can be monomethylated, and results in 1-methyladenosine (m1A) or N6methyladenosine (m6A), which are the two most common RNA modifications in eukaryotes. The methyl group makes up only 5% of the molecular mass of m1A or m6A. Therefore, it has been challenging to distinguish the two isomeric ions by using the current ion mobility techniques. If the size of those methylated ribonucleosides is reduced by cutting off the ribose, the same methyl group would make up 10% of the remaining molecular mass. Therefore, the proposed size reduction is equivalent to amplifying the influence from the methyl group (or other RNA modifications) on the resulting molecular shape. From the perspective of IMS, the smaller the ions that can be generated through size reduction, the bigger the difference can be generated in the molecular shapes between two isomeric ions. To evaluate this concept, the collision cross section (CCS) of m1A and m6A with or without removing the ribose was calculated. The results are summarized in Table 1. By cross checking the calculated CCS value of m1A with the experimentally measured CCS values in the unified CCS compendium, the CCS calculations in Table 3 were determined to be accurate. More importantly, the results in Table 3 indicate the removal of ribose from m1A and m6A ions would theoretically lower the required resolution for differentiating the two selected isomers by 16% (Table 3). In other words, it becomes easier to resolve the smaller methylated adenine ions than the corresponding larger methylated adenosine ions.

Table 3. Comparison of collision cross section (CCS) and minimum resolution (R) that is required to resolve the peaks of selected isomeric ions in an ion mobility spectrum.

Isobaric Ions	Calculated CCS (Å ²)	Required Resolution
m1A	164.1	36.67
m6A	168.7	
m1a	124.7	30.69
m6a	128.9	

Theoretically, the glycosidic bond between the nucleobase and the ribose sugar within the molecular structure of ribonucleotides is relatively weak. According to the earlier reports, the dissociation of the N-glycosidic bond did occur frequently under the normal collision-induced dissociation (CID) conditions of MS/MS experiments, and led to a neutral loss of the ribose while the positive charge remained on the nucleobase ions.⁴⁹ Since the nucleobase has been the target for majority of the known RNA modifications,⁵⁰ the loss of the ribose does not represent any significant drawback to the proposed sizedreduction ion mobility (SRI) method.

In this study, all IM measurements were carried out on a highly flexible IM platform named Waters Synapt G2, which is equipped with the traveling wave ion mobility (TWIM) technology and allows accurate mass spectrometric measurements to be carried out simultaneously.⁵¹ In order to simplify our study, the selected ribonucleoside standards were directly infused into the instrument via an electrospray ionization source. Depending upon the

⁴⁹ Ham and MaHam, *Analytical Chemistry: A Chemist and Laboratory Technician's Toolkit*.

⁵⁰ Boccaletto et al., "MODOMICS: A Database of RNA Modification Pathways. 2017 Update."

⁵¹ Giles, Williams, and Campuzano, "Enhancements in Travelling Wave Ion Mobility Resolution."

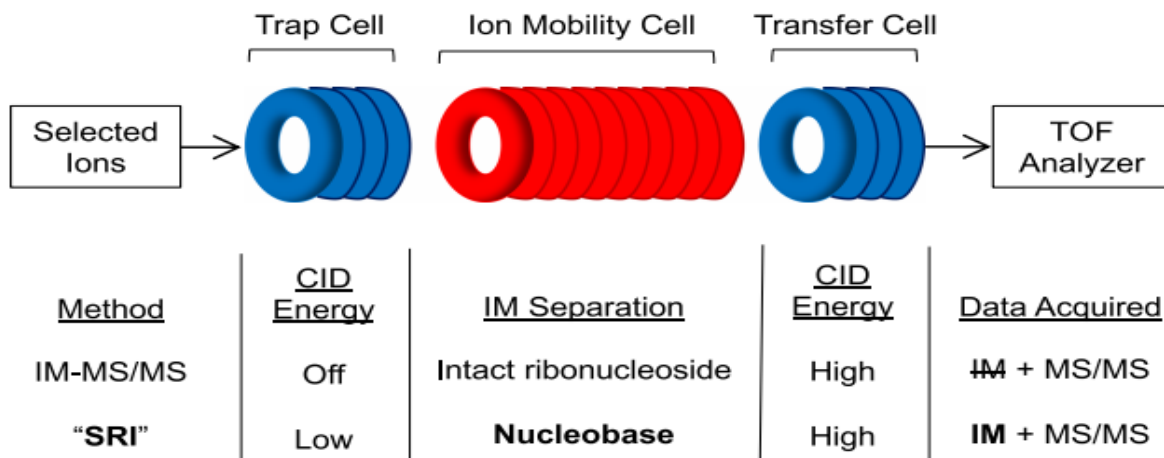
actual sample complexity, the deviation from the standard approach of using liquid chromatography to separate the ribonucleosides prior to MS or IM-MS measurements is theoretically feasible and has been reported.⁵² As indicated in Fig. 13, prior to the IM separation, ions with specific mass-to-charge ratios (m/z) are selected by a quadrupole mass filter. In order to convert the continuous flow of ions exiting from the quadrupole into batches of ions for TWIM, a trap cell is inserted in between the quadrupole and the IM cell (Fig. 13). At the rear end of the IM cell, there is also a transfer cell. By increasing the voltage at the entrance of the trap or transfer cell, the ion energy can be increased, and leads to the collision-induced dissociation of ions. Under the default operations for IM measurements, the CID of ions is normally set up to occur in the transfer cell after the IM separation is completed (Fig. 13). In order to maximize the yield of different CID fragment ions, there is an option to carry out CID in both trap and transfer cells. For structural analysis, the dual CID approach is referred as time aligned parallel (TAP) fragmentation.⁵³ In the TAP analysis, the resulting CID fragment ions in the trap and transfer cells are aligned through their arrival time distribution (ATD). The experimental approach of our proposed method is similar to the TAP analysis, in which the selected ions are dissociated in both trap and transfer cells. In contrast to the TAP analysis, our proposed method aims to reduce the size of the precursor ions by carrying out a very limited ion dissociation in the trap cell; thus, the minimum amount of CID energy is used to avoid the generation of multiple CID fragment ions. In addition, our proposed method does not require any time aligned parallel fragmentation to identify the isomeric ions. Generally speaking, the approach of reducing the size of isomeric

⁵² Rose et al., "Profiling Ribonucleotide Modifications at Full-Transcriptome Level: A Step toward MS-Based Epitranscriptomics," 2015.

⁵³ Damen et al., "Electrospray Ionization Quadrupole Ion-Mobility Time-of-Flight Mass Spectrometry as a Tool to Distinguish the Lot-to-Lot Heterogeneity in N-Glycosylation Profile of the Therapeutic Monoclonal Antibody Trastuzumab."

ions in the trap cell is equivalent to a step of processing the sample ions before the IM measurements are carried out.

Figure. 13 Schematic diagram of the key components in Waters Synapt G2 that are involved in the ion mobility (IM) measurements and the developed SRI method.



Comparison of parameter settings of the key components and outcomes under the standard IM measurements with tandem mass spectrometry and the SRI method are shown. The novelty of the SRI method is highlighted with bolded font. TOF, time-of-flight; CID, collision-induced dissociation; IM, lack of resolution

For the proof of concept of the SRI method, two of the isomeric methylated adenosine (m1A and m6A) are used as our initial model. As shown in Fig. 14A, despite of our initial efforts to optimize the key parameters of TWIM, namely, the height and the velocity of traveling waves, the two isomeric methylated adenosine ions remain unresolvable, i.e., equal arrival time distribution (ATD). Although slightly higher ion mobility resolution was reported for measuring isomeric RNA modifications, it does not hinder the development of the proposed SRI method. As shown below, the results in Fig. 14A simply serve as a reference in this study. To set up the SRI method, optimal CID energy in the trap cell is required. The results indicated that the default setting at 4 V of CID energy was sufficient to achieve a complete dissociation of the N-glycosidic

bond in both selected methylated ribonucleoside ions. In Fig. 14B, by using the SRI method, the ATD of the two smaller methylated adenine ions (m1a vs m6a) are distinguishable from each other when the same TWIM parameter settings as in Fig. 2a were used. Based on the difference between ATD, the N6-methyladenine (m6a) ion is expected to have a larger CCS than the 1methyladenine (m1a) ion. This observation complies with their calculated CCS values as shown in Table 3. To ensure the ATD measurement of m6a ion is repeatable, fresh m6A samples were prepared on three different days and the IM measurements were repeated at least three times on each day.

Figure 14. A. Molecular structure of m1A and m6A, and their corresponding extracted ion mobility spectra which were acquired by using the standard IM method. B. Molecular structure of m1a and m6a, and their corresponding extracted ion mobility spectra which were acquired by using the SRI method. A, adenosine; a, adenine.

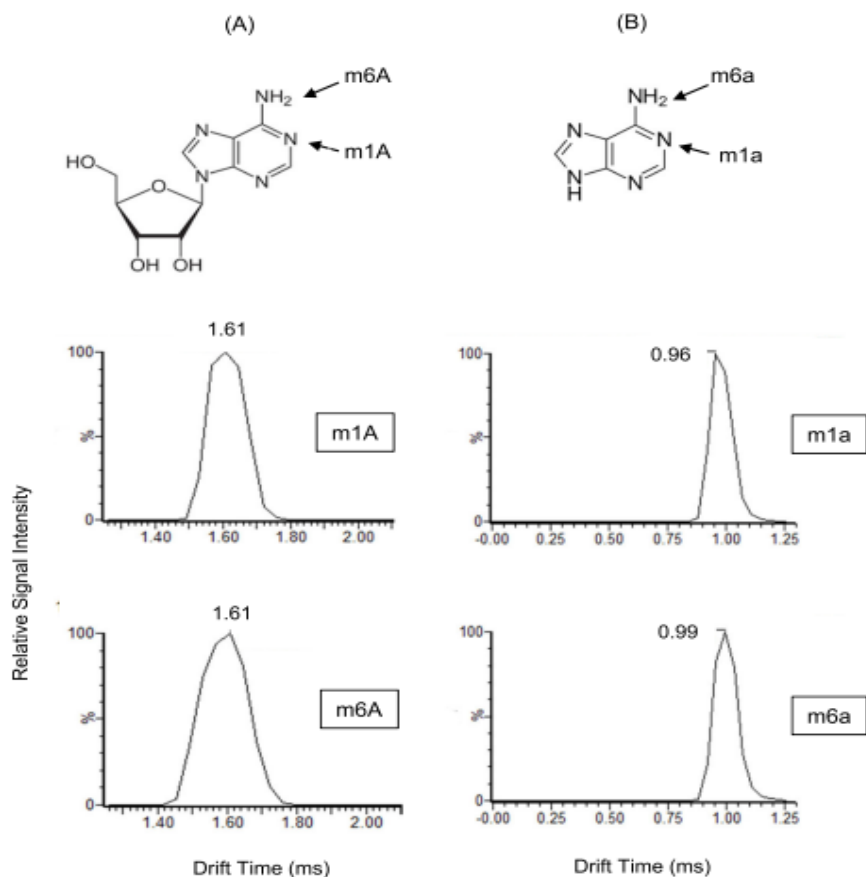
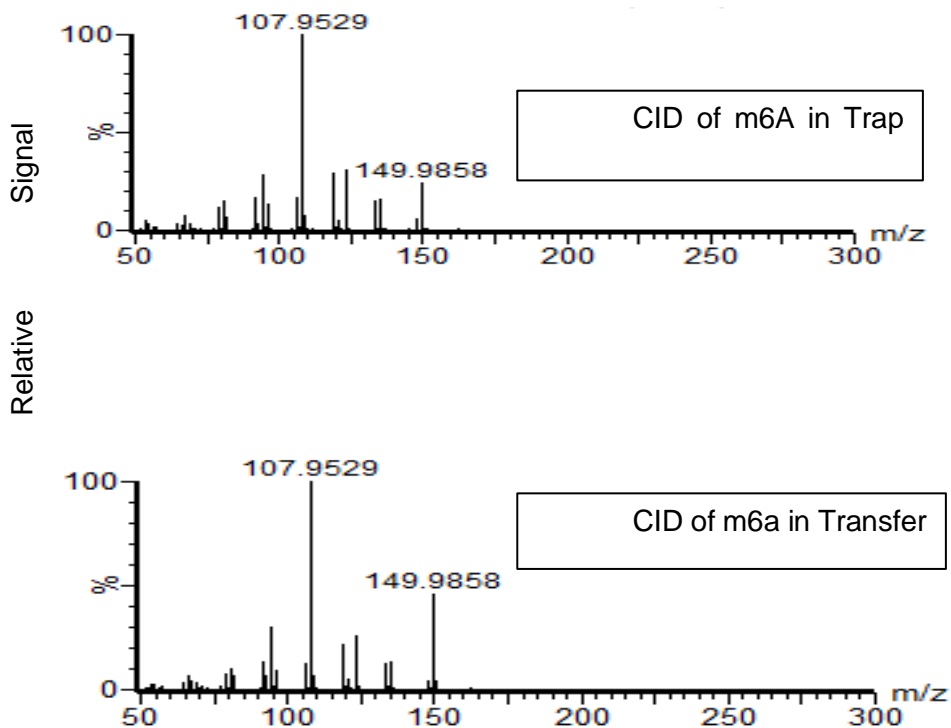


Figure 15. MS/MS spectrum of m6A in the trap cell under the standard MS/MS method or m6a in the transfer cell under the SRI method.



As shown above, the ATD measurements could provide a mean to identify the selected isomeric RNA modifications. However, in order to achieve a higher accuracy, the post-IM MS/MS measurements of the smaller ions are needed.

By default, the trap cell is the designated CID cell for MS/MS experiments. However, when using the SRI method, the transfer cell is the only option for carrying out the MS/MS experiments (Fig. 13). Although the transfer cell has the same design and dimension as the trap cell, their parameter settings are different. Furthermore, based on the results in our earlier study, the internal energy of precursor ions was found to be elevated when the stacked rings ion guides

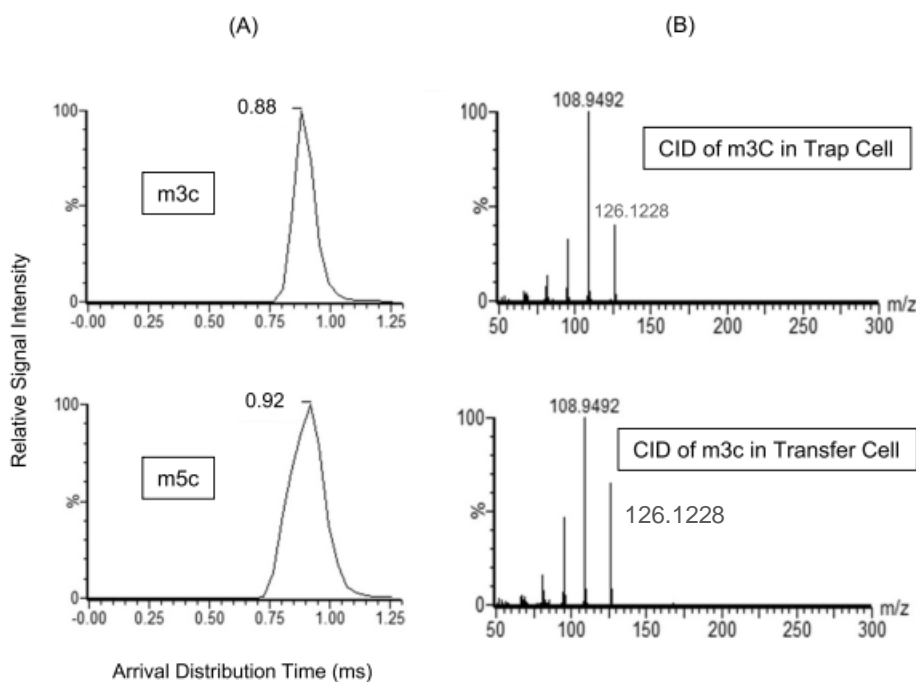
were used to transmit ions in the Waters Synapt G2 instrument (Mwangi 2018). Owing to these reasons, the effectiveness of using the transfer cell to carry out the MS/MS experiments was investigated. After optimizing CID energy, the spectral pattern obtained from using the transfer cell to fragment the m6a ions was found to match with the results obtained from using the trap cell to fragment the m6A ions under the standard MS/MS mode

In the latter case, (Fig. 15) due to the use of relative high CID energy (80 V), the precursor ion of m6A was not detectable and only the methylated adenine ion (149.99 m/z) was detected. With similar level of signal intensity in both MS/MS spectra shown in Fig. 4, it represents that there is no compromise on using the SRI method in comparison to the standard MS/MS method. Together with the ATD results in Fig. 14B, it demonstrates the SRI method is a viable approach to distinguish the two selected isomeric RNA modifications with higher accuracy than the standard MS/MS method.

Application of SRI method to other isomeric RNA modifications

To demonstrate its applicability, the SRI method was also used to detect and distinguish the most common isomeric modification of cytidine, namely, 3methylcytidine (m3C) and 5-methylcytidien (m5C). Through the size reduction of their corresponding precursor ions as described above, a unique and reproducible ATD could be measured for each dissociated cytosine ions (m3c vs m5c) without any further optimization of the parameter settings. The results are shown in Fig. 16A. In comparison to the results obtained from the analysis of m1a and m6a ion in Fig. 14B, there is a slightly bigger difference in ATD between m3c and m5c ion. This is attributed to cytosine that has a smaller size than adenine.

Figure 16. A. Extracted ion mobility spectra of nucleobases that resulted from using the SRI method. B. MS/MS spectrum of m3C in the trap cell under the standard MS/MS method or m3c in the transfer cell under the SRI method. The CID energy used in the trap and transfer cell was 80 V and 140 V, respectively. The ion counts for 108.9492 m/z ion in both cases reached 5e+4 and 4e+4, respectively. m3c, methylcytosine; m5c, 5-methylcytosine; m3C, 3-methylcytidine



To complete the analysis, the MS/MS measurements of m3c and m5c ions were carried out. A unique CID fragment ion with m/z of 95.01 was easily detectable from the precursor ion of m3c, which could be used to distinguish the two isomeric compounds. As indicated in Fig. 16B, the results obtained from the CID of m3c ion in the transfer cell under the SRI method is comparable to the results that were obtained from the CID of m3C ion in the trap cell under the standard MS/MS mode. Thus, the SRI method does support acquiring the same level of structural

information as in the case of using the standard MS/MS method while enriching the data set with the ATD of the dissociated nucleobase ions.

Overall, the results in Fig. 16 demonstrate the SRI method can be used to detect and distinguish other isomeric RNA modifications.

Although quantitative mass spectrometry has already been extended to the analysis of many RNA modifications including RNA methylation,^{54,55,56} the effectiveness of using the Waters Synapt G2, in which ion mobility spectrometry is coupled to mass spectrometry, for performing quantitative analysis of RNA modifications especially under the SRI method is unknown. In order to ensure the SRI method can be applied to determine the level of specific RNA methylation, the calibration experiments with the standard dilution of m6A and m3C were carried out. Since both ATD and MS/MS measurements are included in the SRI method, the calibration can be carried out in two different ways. The results are shown in Fig. 6. In the case of using m6A as the calibrant, the MS/MS measurements were calibrated with the signal corresponding to the methylated adenine ion at 149.99 m/z. The reason for choosing this particular CID fragment ion is because there is no unique CID fragment ion that can be used to distinguish the two selected isomers of methylated adenosine. To overcome this issue, Limbach and his associates had used the ratio of signal intensities between methylated adenine ion (149.99 m/z) and another CID fragment ion (107.95 m/z) that has a higher signal to distinguish the two isomers. Since the detection of both signals were required, the MS/MS calibration with m6A was performed by using the lower signal at 149.99 m/z. In the case of using m3C as the

⁵⁴ Huber et al., “The Versatile Roles of the tRNA Epitranscriptome during Cellular Responses to Toxic Exposures and Environmental Stress.”

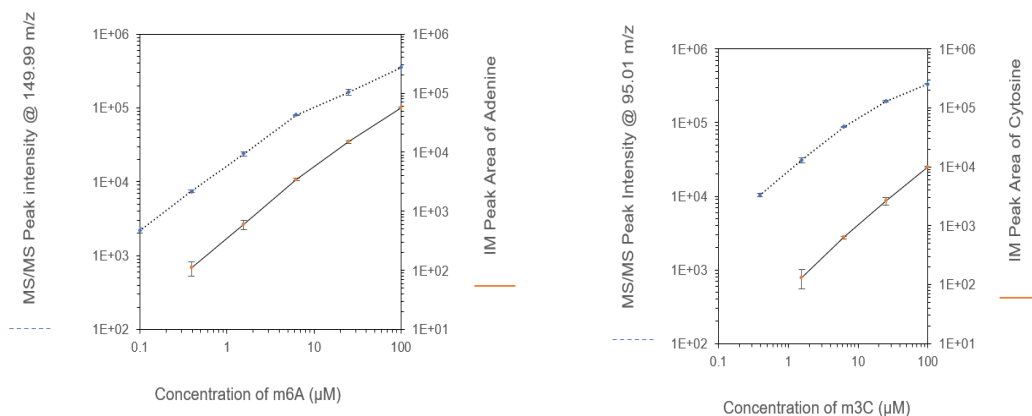
⁵⁵ Collin and Limbach, “Mass Spectrometry of Modified RNAs: Recent Developments (Minireview).”

⁵⁶ Jora et al., “Differentiating Positional Isomers of Nucleoside Modifications by Higher-Energy Collisional Dissociation Mass Spectrometry (HCD MS).”

calibrant, the signal at 95.01 m/z that corresponded to a unique CID fragment ion of m3C was used. For both MS/MS calibrations, the linear dynamic range has about two orders of magnitude and the R-squared values are equal or above 0.99 (Fig. 17). The limit of detection of m6A is slightly lower than the detection of m3C. This is mainly because the yield of m6A ion was higher than that of m3C ion. By comparing the results in Fig. 17. with those obtained by using the standard MS/ MS mode on the same platform, under which the IM operation was turned off and the CID was carried out in the trap cell instead of the transfer cell, no significant difference on both limits of detection was noticed.

For the IM calibration, the signal that corresponds to the dissociated methylated nucleobase in the ion mobility spectrum was used. Based on the design of the SRI method, the IM signal and the MS/MS signals were acquired simultaneously. Therefore, the IM calibration experiments were carried out at the same time with the MS/MS calibration experiments. The results are also shown in Fig. 17. Due to the wider peaks in the ion mobility spectra, the peak area instead of the peak height was used to plot the calibration graphs in Fig. 17. In both cases, the R-squared values are slightly below 0.99. This could be due to the fact that the yield of the dissociated nucleobase ions became lower when the concentration of the parent ribonucleoside ions reached to the ion capacity of the transfer cell. The results in Fig. 6 show that IM calibration is comparable to the conventional MS/ MS calibration. Overall, we show the SRI method can also be used to determine the amount of specific isomeric RNA methylation.

Figure 17. Calibration graphs of m6A and m3C using the SRI method. The MS/MS data (solid line) of a specific post-IM CID fragment ion or the IM data (dotted line) of corresponding methylated nucleobase are plotted against the concentration of methylated ribonucleoside in standard dilution.



Conclusion

In general, two of the drawbacks of ion mobility spectrometry are the lack of sensitivity and resolution. The development of the SRI method represents a complementary effort to address the limitation on ion mobility resolution. To the best of our knowledge, this is the first report that uses the concept of size reduction of ions to directly address the limitation on resolution. Equally important, in comparison to the standard MS/MS method, no significant decrease on the sensitivity was found when the SRI method was used. Furthermore, the ability to detect the selected isomers with distinguishable ATD represents an extra dimension of data is available for the identification of isomeric RNA modifications. Another advantage of using the SRI method is the acquisition of ATD is independent to the MS/MS measurements. Specifically, the ATD measurements are dependent on whether the optimal CID energy is being used neither during the MS/MS measurements nor the actual time available to acquire sufficient MS/MS signals. From

the perspective of MS/MS measurements, both parameters are often critical and determine whether specific CID fragment ion(s) is detectable or not. The SRI method is expected to be applicable to other types of isomeric compounds. Also, it is technically feasible to adopt the concept of the SRI method on other existing or future IMS platforms, in which different types of ion mobility technology is utilized.

CHAPTER IV: FLOW INJECTION ANALYSIS (FIA)

Introduction

The development of new mass spectrometric methods for epitranscriptomic analysis can potentially improve the confidence of our current GBM study in which LC-MS has become a routine method.⁵⁷ As our study gets deeper, the demand for improving our sample throughput is becoming more urgent. In our GBM study, the analysis of multiple samples resulted from both in vitro and in vivo experiments have become more challenging in terms of the time required to complete all the biological and analytical replicates. The current LC-MS method requires a 25-minute run time for each sample injection and another 25-minutes for column washing in between two sample injections. Together with 3 biological replicates and 3 analytical replicates for each sample, it would require about 9 hours of instrument time for every single sample. It was acceptable at the early stage of our GMB study, but obviously not affordable for our future work. The relative long elution profile, the consumption of less environmental friendly mobile phase, and the high cost on the instrument time and labor intensiveness are holding back our research greatly.

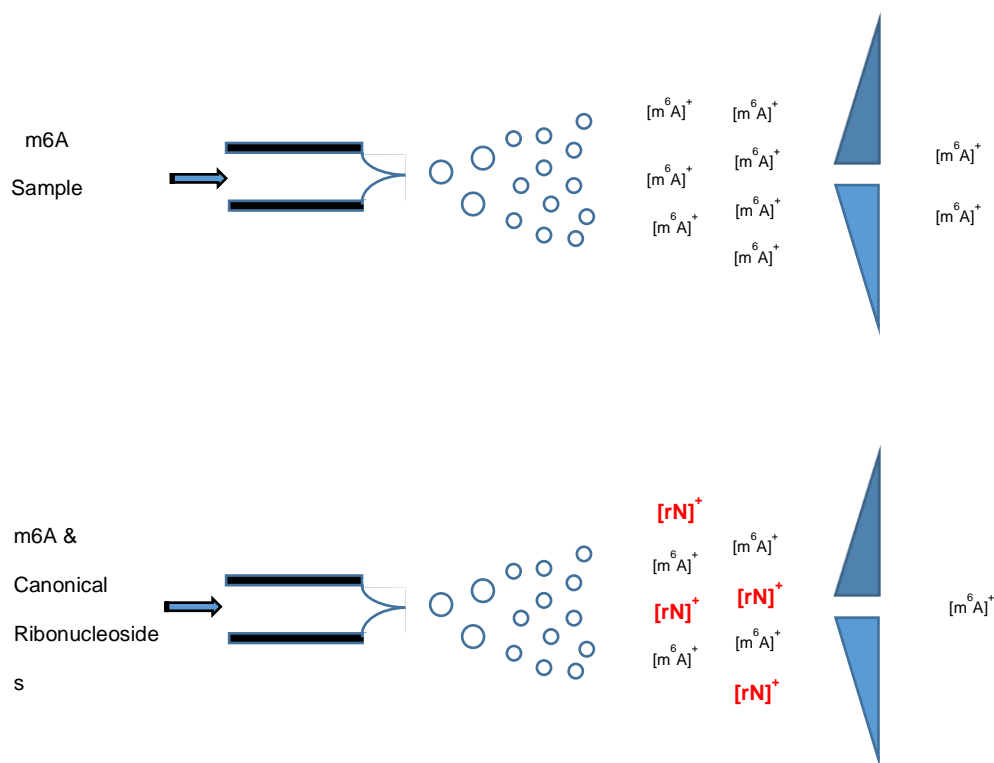
After achieving higher accuracy with our SRI method, another unconventional approach to improve the current LC-MS method takes advantage of the MS capability to perform a targeted analysis in significantly less than 1 second. In a chromatography-free flow injection analysis (FIA) method, a sample of interest with a short list of targeted RNA modifications is directly injected into the mass spectrometer. The analysis time of each sample can be reduced to 2 minutes, and the wash time is limited to 3 mins. In comparison to the total time of 50 minutes

⁵⁷ Alfardus et al., “Intratour Heterogeneity in MicroRNAs Expression Regulates Glioblastoma Metabolism.”

(25 minutes run time and 25 minutes wash time) in our current LC-MS method, the use of FIA method represents a **10-fold saving in time**.

However, there are 4 major challenges for the FIA method. Firstly, one important function of LC column is to separate the chemicals from a complex sample and elute the component one at a time.⁵⁸ Without the column separation, all the chemicals would all be injected into the electrospray (ESI) ion source, thus more ion suppression as shown in Figure 18. Therefore, the lower ion signals would normally be expected.

Figure 18. Ion suppression schematic.



Another challenge for FIA method is the background noise from ESI. In other words, the sensitivity issue.⁵⁹ A big advantage of LC technology is when the column is separating chemicals from mixture sample, it also purifies the sample, so the background noise could be reduced

⁵⁸ Annesley, "Ion Suppression in Mass Spectrometry."

⁵⁹ Neffling et al., "LC-ESI-Q-TOF-MS for Faster and Accurate Determination of Microcystins and Nodularins in Serum."

compared to directly inject mixture into ESI. Therefore, it will required fully optimization for the ESI setting and the solvent to increase the sensitivity of samples. In this way, the sensitivity improvement would offset the background noise increment when switch LCMS to FIA.

The difficulty of applying the FIA method to epitranscriptomic analysis is the identification of isomeric RNA modification.⁶⁰ The common LC-MS methods combine the use of chromatographic data to support the identification of MS data (both MS and MS/MS). In the FIA case, different strategies need to be applied to differentiate the isomers.

After overcoming all technical difficulties as discussed above, the Tris buffer in the digestion of total RNA is known to suppress the ESI ion signals. During the RNA digestion, enzymes must be kept under specific pH. Therefore, to solve this problem, an appropriate approach would be required to identify suitable substitute of Tris buffer for digesting the total RNA samples while being fully compatible to the ESI process.

By considering all four challenges, a fully optimized FIA method was developed for epitranscriptomic analysis using the top three upregulated RNA modifications in GBM epitranscriptomes as our model.

Materials and methods

Adenosine (A), Uridine (U), Guanosine (G), Cytidine (C), 3-methylcytidine (m3C) 5-methylcytidine (m5C), N6-methyladenosine (m6A), N6-Threonylcarbamoyl adenosine (t6A), and N6-methyl-threonylcarbamoyl adenosine (m6t6A), were obtained from Sigma-Aldrich (St. Louis, MO, USA). Acetonitrile (ACN), ethanol, isopropanol, t-butanol, acetic acid, formic acid, and water at the Optima LC/MS grade were purchased from ThermoFisher Scientific (Hampton,

⁶⁰ Li and Limbach, "Identification of RNA Sequence Isomer by Isotope Labeling and LC-MS/MS."

NH, USA). All the stock solution (5 mM) of unmodified and modified ribonucleoside were prepared with deionized water and stored at $-20\text{ }^{\circ}\text{C}$.

LNZ glioblastoma cells were cultured in DMEM medium. (Include fetal bovine serum) Incubation under 37-degree Celsius temperature with 5% CO₂ for 5 to 6 days.

Extraction of RNA

Cells were pelleted and resuspended in 1 mL RNAProtect Bacteria Reagent (Qiagen Inc, Valencia). The cells were washed twice with 1X PBS and pre-lysed with 250 μL 50 g/L lysozyme and 120 μL 1000 units/mL mutanolysin. Total RNA was extracted using the RNeasy mini kit (Qiagen Inc, Valencia). Total RNA samples were DNase-treated twice, and the absence of genomic DNA was confirmed by PCR.

Each RNA sample was digested in an enzymatic reaction of 25 μL at 37 $^{\circ}\text{C}$ for 3 hours, which contained 5 μg rRNA-depleted RNA, 0.05 units phosphodiesterase I, 0.5 units alkaline phosphatase, 5 units benzonase, 50 mM Tris-HCl (pH 8.0) or ammonium bicarbonate (pH 8.0), 1 mM MgCl₂ and 0.1 mg/mL BSA [14]. After removing the enzymes with 3K MWCO spin filter at 14,000g for 15 mins (Pall Corporation, Port Washington, NY), the digested RNA sample was diluted in deionized water to 50 ng/ μL .

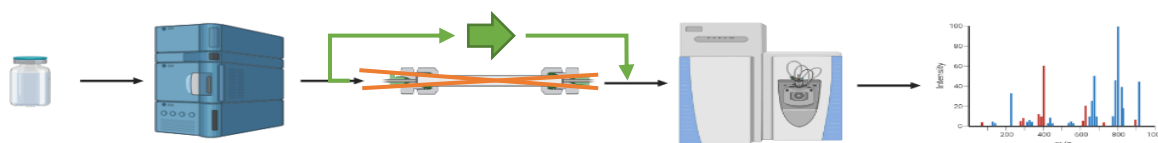
An Acquity ultra-high performance liquid chromatography (UPLC) system (Waters Corporation, Milford, MA) which was equipped with an Acquity HSS T3 column (2.1 x 50 mm, 1.8 μm) and a HSS T3 VanGuard pre-column (2.1 x 5 mm, 1.8 μm) at 30 $^{\circ}\text{C}$ was used. After injecting 10 μL of sample, the elution was carried out with a binary solvent system, in which solvent A contained water and 0.01 % (v/v) formic acid, and solvent B contained 50 % acetonitrile and 0.01 % (v/v) formic acid at a flowrate of 0.4 mL/min. The gradient elution profile initiated at 100:0 (A:B) from 0.0 – 0.5 min., ramping to 70:30 from 0.5 – 9 mins, followed by 50:50 from 9 –

10 mins, and ended with 0:100 from 10 – 17 mins. Randomized injections were used. The negative control was prepared without any RNA sample.

Tandem mass spectrometry (MS/MS) was performed on a Q Exactive Plus (ThermoFisher Scientific, Waltham, MA) in the positive mode with ESI at 425 °C and 3.5 kV. Sheath and auxiliary gas flow were at 50 and 13 arbitrary units, respectively. Data were acquired with an inclusion list of calculated m/z of all known RNA modifications. The mass calibration was performed using a canonical ribonucleoside standard mixture (6.5/μM). Data analysis was carried out with Xcalibur (ThermoFisher Scientific, Waltham, MA) restricting the precursor ion to ≤ 5 ppm accuracy and its retention time to ≤ 0.1 min.

Same samples were delivered by the UPLC system but without the column. The final optimized solvent contained 60% ethanol and 0.1 % (v/v) acetic acid at a flowrate of 0.05 mL/min. Tandem mass spectrometry (MS/MS) was performed on a Q Exactive Plus (ThermoFisher Scientific, Waltham, MA) in the positive mode with ESI at 400 °C and 3.5 kV. Sheath and auxiliary gas flow were at 30 and 10 arbitrary units, respectively.

Figure 19. Workflow of FIA method.

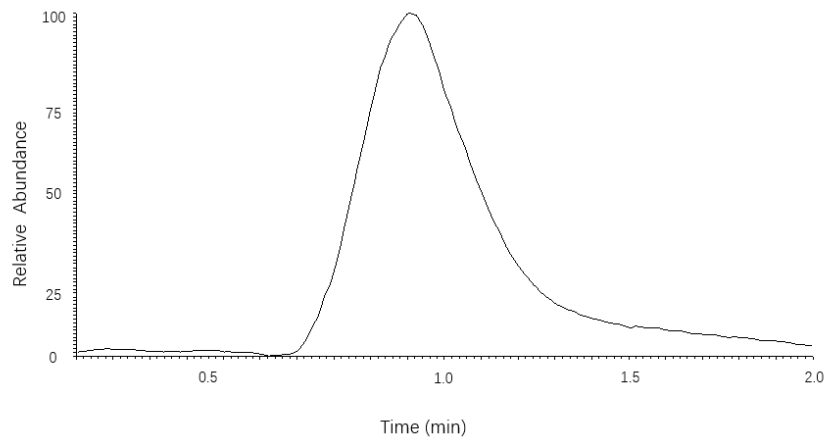


R

The flowrate setting was minimized in order to enhance the signal intensity while extending the time for acquiring the signals. It provided about half a minute of decent signals for both qualitative and quantitative analysis. According to the manufacturer, the time required for Q Exactive MS instrument to complete a scan of one targeted ion is only 64 milliseconds. In other

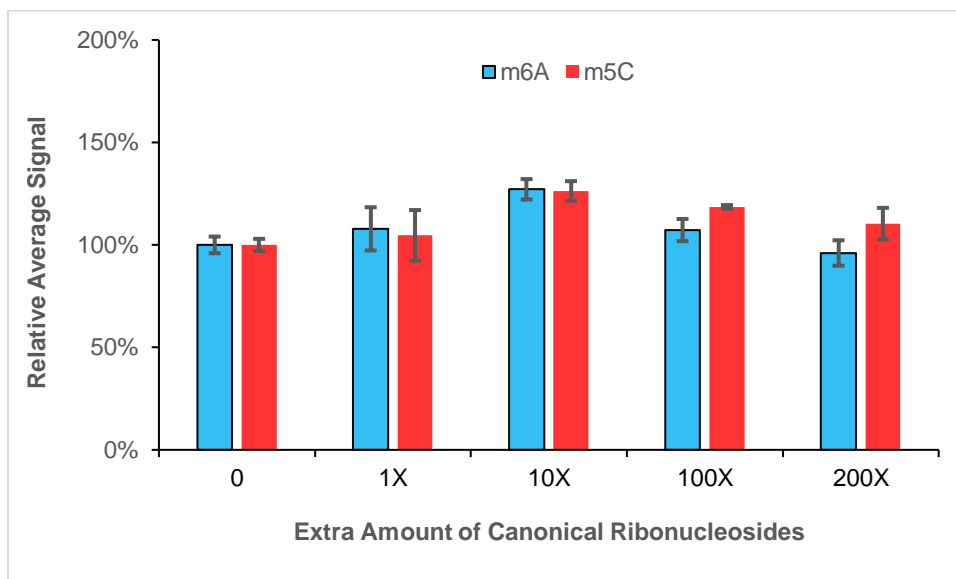
words, it means within the half-minute window >100 different RNA modifications can be detected, which is many than enough for any epitranscriptomic analysis.

Figure 20. The representative ion chromatogram of a selected canonical ribonucleoside ion showing the available time window for acquisition.



The ion suppression does theoretically exist, thus the level of ion suppression was the first priority to be figured out.

Figure 21. Evaluation of ion suppression in the electrospray ionization source.



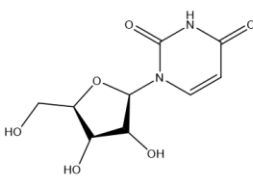
Bar chart showing the results from measuring 0.65 μ M of selected modified ribonucleosides (m6A or m5C) with various extra amounts of canonical ribonucleoside standards present in the same sample. All four canonical ribonucleosides are present in equal amounts. 50% acetonitrile was used as the mobile phase. The average signal of each specific ribonucleoside was referenced to its corresponding average signal without the presence of any canonical ribonucleosides. Each error bar represents one standard deviation ($n = 3$).

The ion suppression test shows that the two modify ribonucleosides did not lose any signal intensity even under the presence of 100 times of canonical ribonucleosides (100X is the total amount of sample injected in the standard LC-MS method). Therefore, the ion suppression would not affect the FIA method.

The profiling of GBM cells includes 32 different RNA modifications, 17 of them are isomers. Some of the isomeric ribonucleoside ions could be simply identified by their unique CID fragment ions. For example, the Uridine and Pseudouridine. Uridine has a unique CID peak at 113.0346 m/z and Pseudouridine has a unique CID peak at 155.0448 m/z.

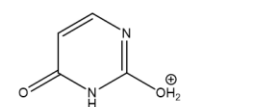
Figure 22. Identification of isomeric ribonucleoside ions.

Mass [m/z]	Formula [M]	modification
282.1202	C11O4N5H15	m1A,Am,m6A
258.1089	C10O5N3H15	m3C,m5C,Cm
259.0930	C10O6N2H14	m5U,m3U,Um,m1Y
298.1151	C11O5N5H15	m1G,m2G,m7G,Gm
296.1358	C12O4N5H17	m6Am,m6,6A
245.0773	C9O6N2H12	Y
245.0773	C9O6N2H12	U
269.0885	C10O5N4H12	I
286.1039	C11O6N3H15	ac4c
247.0930	C9O6N2H14	D
346.1250	C13O8N3H19	acp3U
283.1042	C11O5N4H14	m1I
326.1464	C13O5N5H21	m2,2,7G
273.1086	C11O6N2H16	m5Um
427.1577	C16O8N6H22	m6t6A
336.1671	C15O4N5H21	i6A
312.1307	C12O5N5H17	m2,2G
459.1298	C16O8N6H22S1	ms2t6A
268.1048	C10O4N5H13	A
284.0997	C10O5N5H13	G
244.0935	C9O5N3H13	C
333.0755	C12O7N2H16S1	mcm5s2U
413.1420	C15O8N6H20	t6A

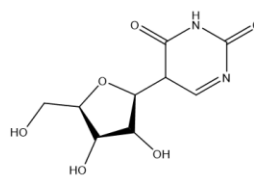


Uridine

↓ CID

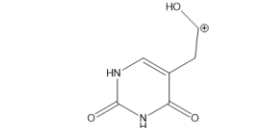


m/z= 113.0346



Pseudouridine

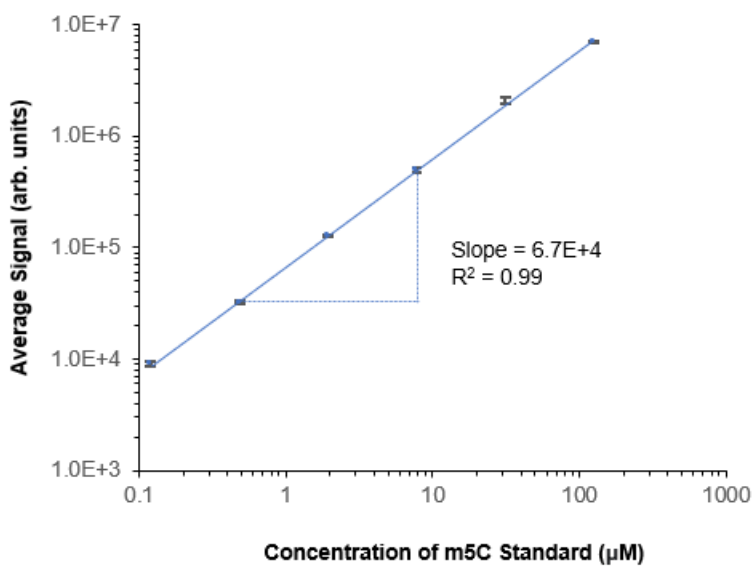
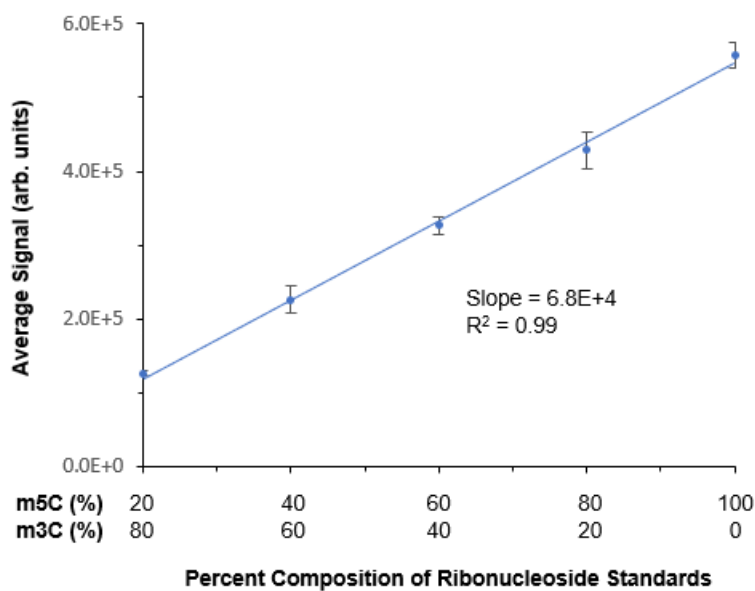
↓ CID



m/z= 155.0448

However, some of the isomers do not have any unique CID fragment ions. For example, m5C modification, one of the important targets in our GBM model. It has the same CID fragmentation pattern as m3C. The solution for differentiating those isomers is by using the relatively high signal intensity of m5C in comparison to the lower signal intensity of m3C. The fragment ion at 108.558 m/z was chosen. Under the same precursor ion concentration, the signal intensity of this fragment ion from m5C is ~20 times higher than that of m3C. To demonstrate the feasibility of using this approach to distinguish the two isomeric modifications, two calibration curves of this fragment ion have been constructed, one was based on pure m5C standard alone, and the other one contained different percentage of m3C in the sample.

Figure 23. Determination of the quantity of m5C modification.



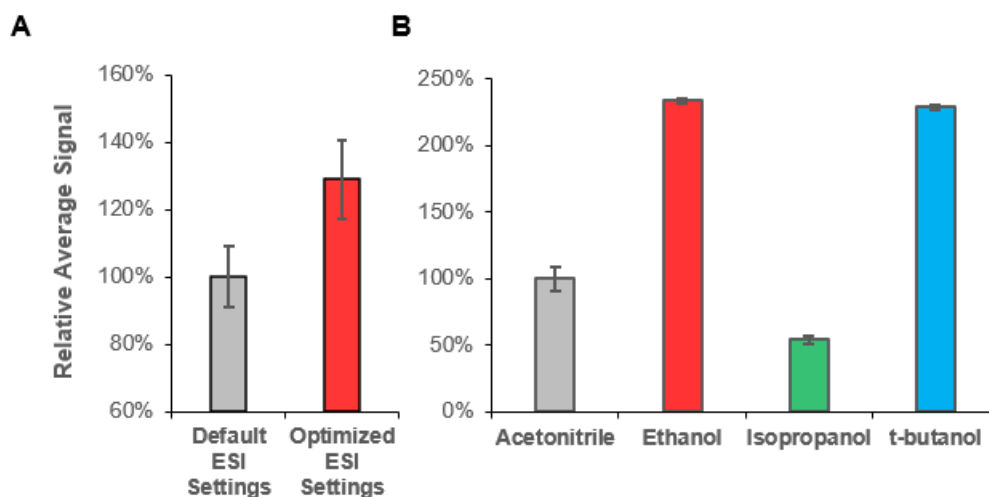
(A) Scatterplot showing the signal variation of a CID fragment ions (108.558m/z) corresponds to the composition of m5C ribonucleoside in a binary standard mixture with m3C ribonucleoside. 100% m5C is equal to 7.81µM of m5C. Each error bar represents one standard deviation (n = 3). (B) Calibration curve that was performed with the standard dilutions of m5C

ribonucleoside alone. The average signal of the same CID fragment ion was used to plot the calibration curve. The slope values were obtained from linear regression analysis, and the R-squared values are as shown in the figure.

The almost identical slope value means the presence of m3C in the binary standard mixture does not interfere with the quantitation of m5C.

Without the limitation from the LC column, any kind of solvent can be applied to this method. The optimization of solvent could greatly improve the sensitivity of the FIA method. The solvent optimization started with the base solvent, namely 50% acetonitrile, that was used as the mobile phase in our established LC-MS method.

Figure 24. Optimization of solvent chosen.



(A) Bar chart showing the results from using different parameter settings for carrying out the electrospray ionization (ESI) to measure an equal molar mixture of canonical ribonucleosides (4 μ M). The average signal of canonical ribonucleoside was referenced to the average signal obtained from using the default settings, which were defined by the sample flowrate (50 μ L/min).

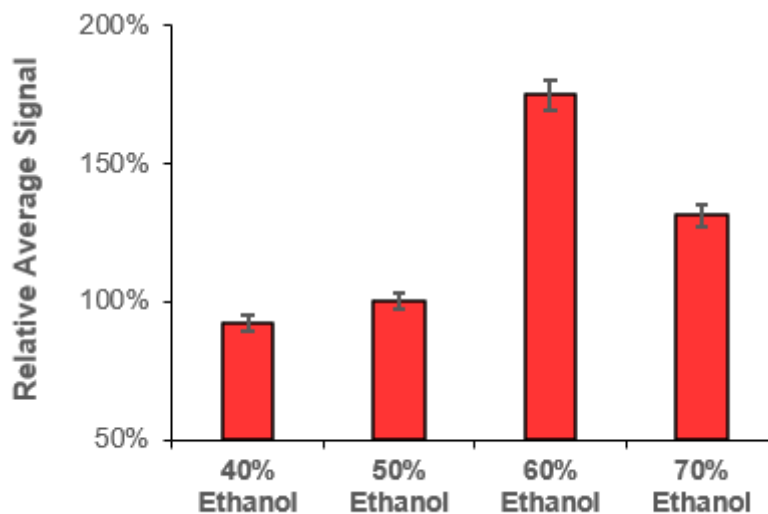
(B) Bar chart showing the results from using different mobile phases to inject the canonical ribonucleoside mixture. For each mobile phase, 50% (v/v) of the selected solvent was used. The

average signal of canonical ribonucleoside was referenced to the average signal obtained from using acetonitrile as the mobile phase.

Table 4. Table of solvent properties that are related to electrospray ionization.

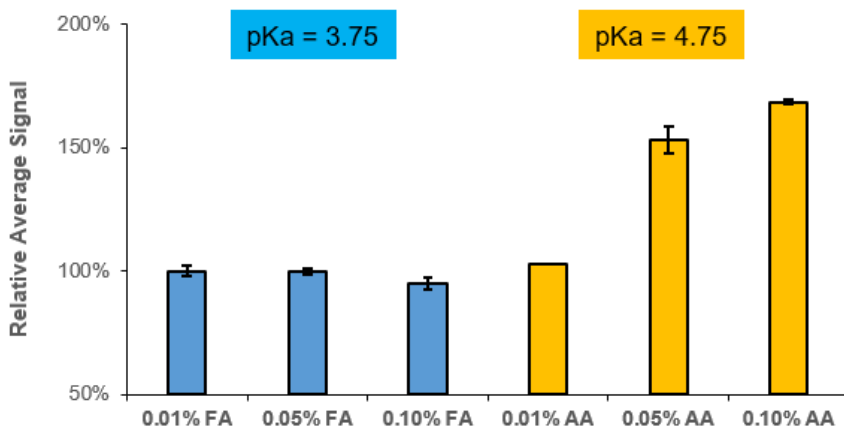
Solvent	Relative Polarity	Boiling Point (°C)	pKa
Acetonitrile	0.46	82	25.0
Ethanol	0.65	79	16.0
Isopropanol	0.55	82	17.1
Tert-butanol	0.39	82	16.5

Figure 25 Optimization of the percentage of ethanol.



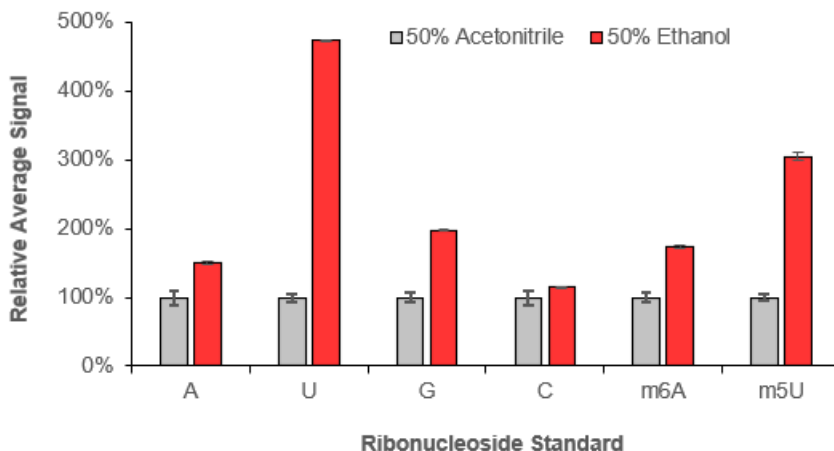
Bar chart showing the results from using different percentages of ethanol as the mobile phase to measure the canonical ribonucleoside mixture. Prior to data acquisitions, the ESI settings were optimized with 50% ethanol. The average signal of canonical ribonucleoside was referenced to the average signal obtained from using 50% ethanol as the mobile phase. Each error bar represents one standard deviation (n = 3).

Figure 26. Optimization of using an acidic additive.



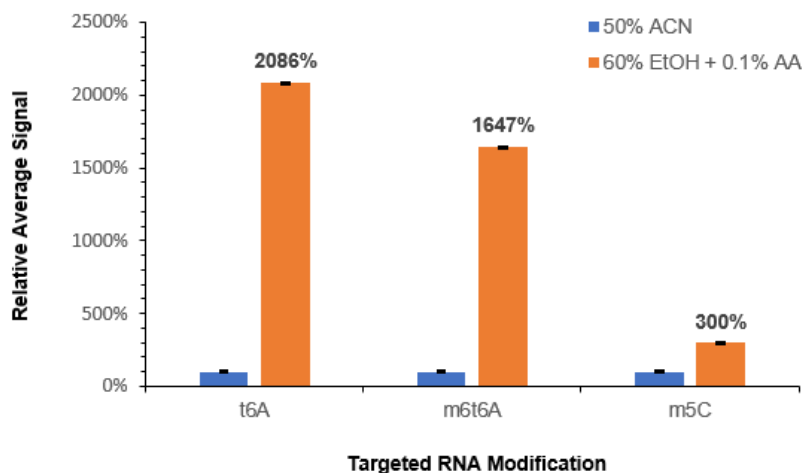
Bar chart showing the results from having different amounts of additive in the mobile phase (60% ethanol). The selected additives include formic acid (FA) and acetic acid (AA). An equal molar mixture of canonical ribonucleosides was measured. The average signal of canonical ribonucleoside was referenced to the average signal obtained from using 0.01% FA. Each error bar represents one standard deviation (n = 3).

Figure 27. Comparing the effects of 50% acetonitrile and 50% ethanol on different ribonucleosides.



Bar chart showing the improvement on ribonucleoside signals that resulted from switching the mobile phase content is dependent on the intrinsic properties of individual ribonucleoside. An equal molar mixture of all six ribonucleosides was measured. The average signal of each ribonucleoside was referenced to the corresponding average signal obtained from using 50% acetonitrile as the mobile phase. Each error bar represents one standard deviation (n = 3).

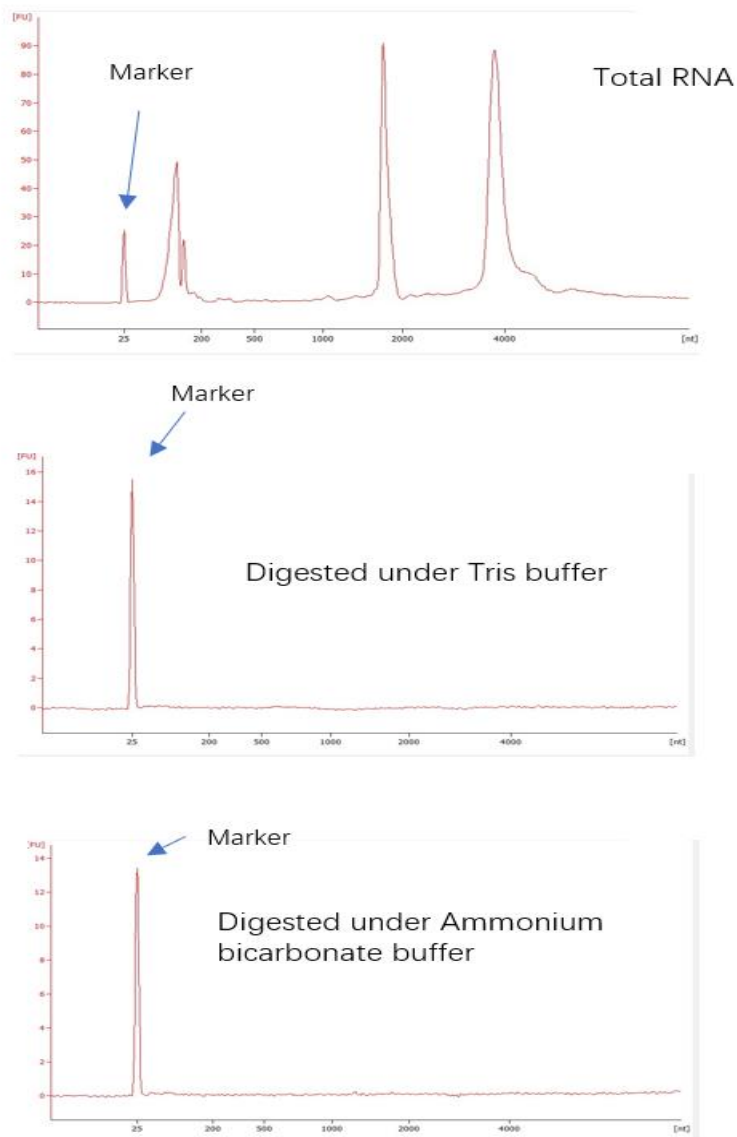
Figure 28. Improvement of signal intensity after optimizing the FIA solvent.



Bar chart showing the final improvement on ribonucleoside signals that resulted from the default 50% acetonitrile solvent of individual target ribonucleoside. An equal molar mixture of t6A, m6t6Am and m5C ribonucleosides was measured. The average signal of each ribonucleoside was referenced to the corresponding average signal obtained from using 50% acetonitrile as the solvent and using 60% ethanol with 0.1% acetic acid. Each error bar represents one standard deviation (n = 3).

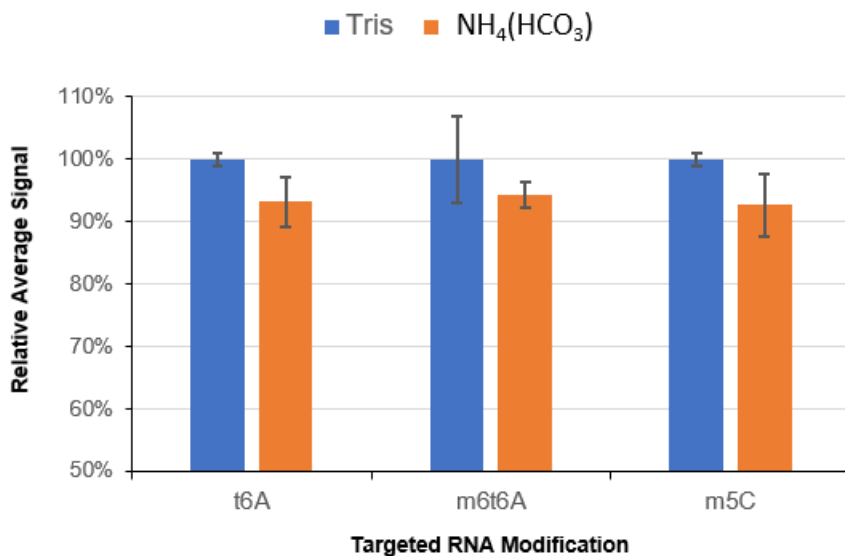
The digestion protocol required Tris as a buffer to maintain pH for the enzyme to work. The new FIA method explored another possibility to use ammonium bicarbonate ($\text{NH}_4(\text{HCO}_3)$) as buffer for digestion. After the digestion process by both Tris buffer and ammonium bicarbonate. The results obtained from both electrophoresis analysis and LC-MS analysis were compared.

Figure 29. Electrophoresis analysis.



The electrophoresis analysis shows that total RNA would have signals within about 50 to 4000 nucleotide range. After digestion process by both Tris buffer and ammonium bicarbonate buffer, all the signal is gone. In other words, both buffer are suitable for the digestion process.

Figure 30. LC-MS analysis.



The individual signal for three main targets has less than 10% difference from using two buffers.

Figure 31. FIA calibration curve with t6A standard.

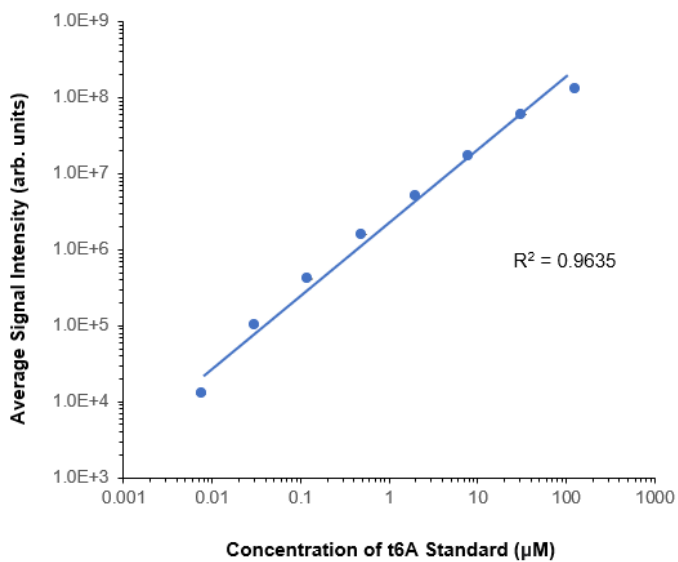


Figure 32. FIA calibration curve with m6t6A standard.

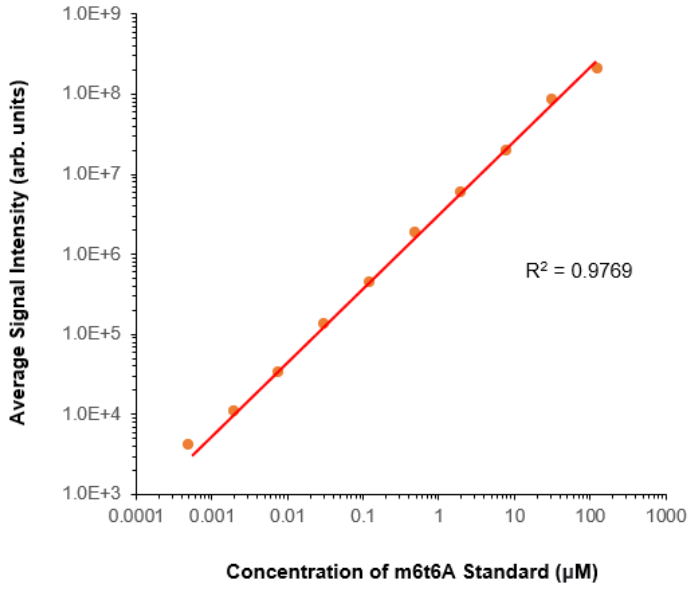
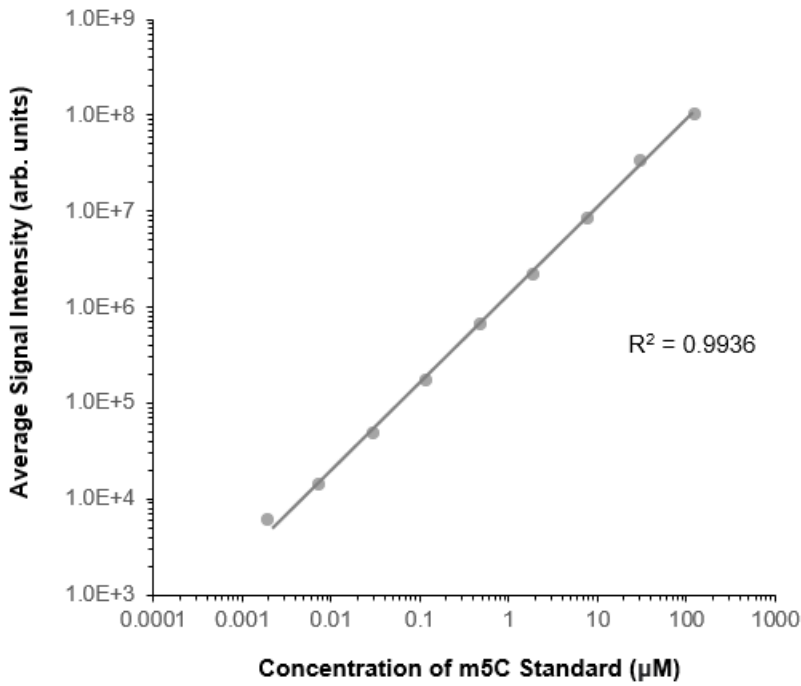


Figure 33. FIA calibration curve with m5C standard.

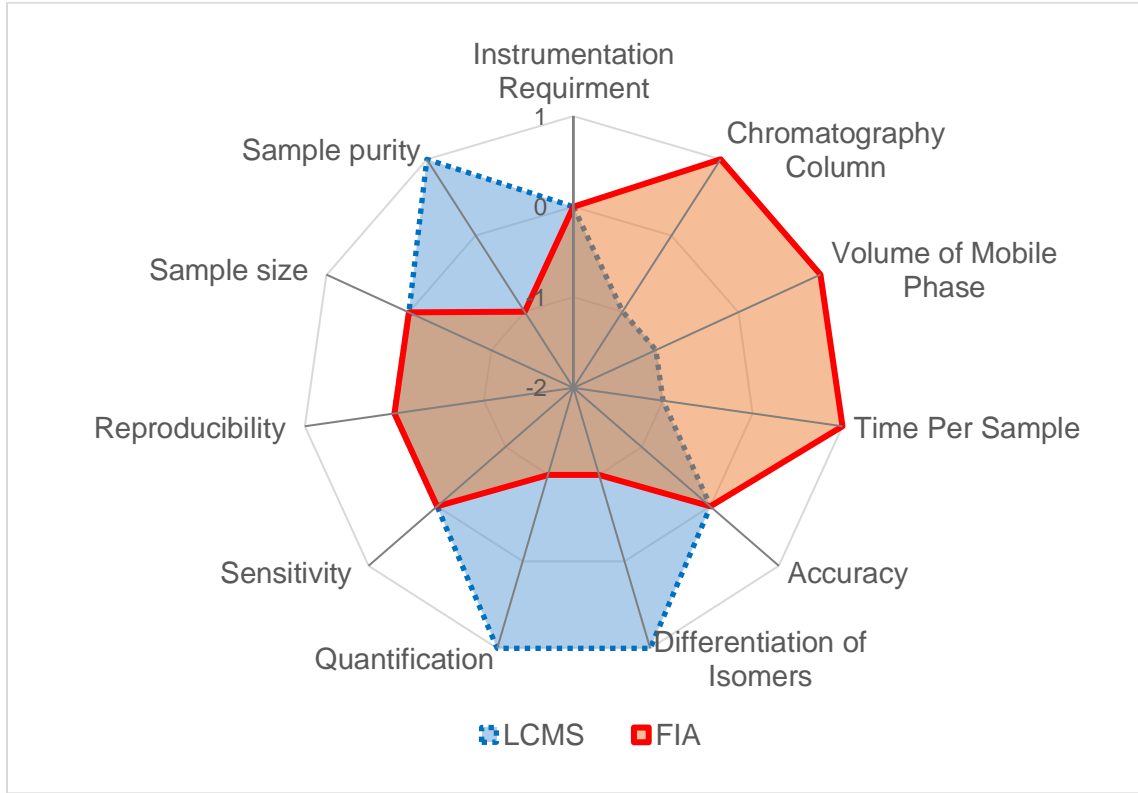


Conclusion

The FIA method could cut down the time spent on each sample 10 times in comparison to the original LC-MS method. The test for ion suppression showed the FIA method has not been significantly impacted by the co-existence of other sample components during the ESI process. The identification of isomer (m5C) which is related to our ongoing GBM studies is achievable. The sensitivity of FIA has been improved by optimizing the solvent being used. Overall, the FIA method was as sensitive as the original LC-MS method. A new buffer that is more compatible with ESI has been explored and the data shows that it is suitable for digestion process. The reason of using ammonium bicarbonate as a new buffer because it would be decomposed into ammonia and carbon dioxide gas.

In conclusion, our results have shown that the FIA method is a viable alternative to LC-MS method for epitranscriptomic analysis. In comparison to the LC-MS method, the FIA method is column free, require less volume of mobile phase, and holds great potential on achieving high sample throughput. Also, it achieved the same sensitivity and sample size as the LC-MS method. The drawback of FIA is that it could not purify the sample due to lack of column, and because of that, it cannot resolve all the isomers.

Figure 34. Advantages and disadvantages between LC-MS and FIA method.



REFERENCES

- Alfardus, Huda, Maria de los Angeles Estevez-Cebrero, Jonathan Rowlinson, Amna Aboalmaaly, Anbarasu Lourdasamy, Salah Abdelrazig, Catherine Ortori, et al. “Intratumour Heterogeneity in MicroRNAs Expression Regulates Glioblastoma Metabolism.” *Scientific Reports* 11, no. 1 (December 1, 2021). <https://doi.org/10.1038/S41598-021-95289-9>.
- Annesley, Thomas M. “Ion Suppression in Mass Spectrometry.” *Clinical Chemistry* 49, no. 7 (July 1, 2003): 1041–44. <https://doi.org/10.1373/49.7.1041>.
- Barbieri, Isaia, and Tony Kouzarides. “Role of RNA Modifications in Cancer.” *Nature Reviews. Cancer* 20, no. 6 (June 1, 2020): 303–22. <https://doi.org/10.1038/S41568-020-0253-2>.
- Basanta-Sanchez, Maria, Sally Temple, Suraiya A. Ansari, Anna D’Amico, and Paul F. Agris. “Attomole Quantification and Global Profile of RNA Modifications: Epitranscriptome of Human Neural Stem Cells.” *Nucleic Acids Research* 44, no. 3 (February 18, 2016). <https://doi.org/10.1093/NAR/GKV971>.
- Bastard, Quentin Le, Guillaume Chapelet, François Javaudin, Didier Lepelletier, Eric Batard, and Emmanuel Montassier. “The Effects of Inulin on Gut Microbial Composition: A Systematic Review of Evidence from Human Studies.” *European Journal of Clinical Microbiology & Infectious Diseases : Official Publication of the European Society of Clinical Microbiology* 39, no. 3 (March 1, 2020): 403–13. <https://doi.org/10.1007/S10096-019-03721-W>.
- Boccaletto, Pietro, Magdalena A. MacHnicka, Elzbieta Purta, Pawek Pitkowski, Blazej Baginski, Tomasz K. Wirecki, Valérie De Crécy-Lagard, et al. “MODOMICS: A Database of RNA Modification Pathways. 2017 Update.” *Nucleic Acids Research* 46, no. D1 (January 1, 2018): D303–7. <https://doi.org/10.1093/nar/gkx1030>.

- Boccaletto, Pietro, Magdalena A Machnicka, Elzbieta Purta, Pawel Piatkowski, Blazej Baginski, Tomasz K Wirecki, Valérie de Crécy-Lagard, et al. “MODOMICS: A Database of RNA Modification Pathways. 2017 Update.” *Nucleic Acids Research* 46, no. D1 (January 4, 2018): D303–7. <https://doi.org/10.1093/nar/gkx1030>.
- Chen, Bei, Bi Feng Yuan, and Yu Qi Feng. “Analytical Methods for Deciphering RNA Modifications.” *Analytical Chemistry* 91, no. 1 (January 2, 2019): 743–56. <https://doi.org/10.1021/ACS.ANALCHEM.8B04078>.
- Collin, Wetzel, and Patrick A. Limbach. “Mass Spectrometry of Modified RNAs: Recent Developments (Minireview).” *Analyst*. 15, no. 1 (2014): 34–48. <https://doi.org/10.1038/nrg3575>.Systems.
- Dalluge, Joseph J., Tetsuo Hamamoto, Koki Horikoshi, Richard Y. Morita, Karl O. Stetter, and James A. McCloskey. “Posttranscriptional Modification of tRNA in Psychrophilic Bacteria.” *Journal of Bacteriology* 179, no. 6 (1997): 1918–23. <https://doi.org/10.1128/JB.179.6.1918-1923.1997>.
- Damen, Carola W.N., Weibin Chen, Asish B. Chakraborty, Mike van Oosterhout, Jeffrey R. Mazzeo, John C. Gebler, Jan H.M. Schellens, Hilde Rosing, and Jos H. Beijnen. “Electrospray Ionization Quadrupole Ion-Mobility Time-of-Flight Mass Spectrometry as a Tool to Distinguish the Lot-to-Lot Heterogeneity in N-Glycosylation Profile of the Therapeutic Monoclonal Antibody Trastuzumab.” *Journal of the American Society for Mass Spectrometry* 20, no. 11 (November 2009): 2021–33. <https://doi.org/10.1016/j.jasms.2009.07.017>.
- Egli, Martin, George Minasov, Valentina Tereshko, Pradeep S. Pallan, Marianna Teplova, Gopal B. Inamati, Elena A. Lesnik, et al. “Probing the Influence of Stereoelectronic Effects on the

- Biophysical Properties of Oligonucleotides: Comprehensive Analysis of the RNA Affinity, Nuclease Resistance, and Crystal Structure of Ten 2'-O-Ribonucleic Acid Modifications.” *Biochemistry* 44, no. 25 (June 28, 2005): 9045–57. <https://doi.org/10.1021/BI050574M>.
- Giles, Kevin, Jonathan P. Williams, and Iain Campuzano. “Enhancements in Travelling Wave Ion Mobility Resolution.” *Rapid Communications in Mass Spectrometry : RCM* 25, no. 11 (June 15, 2011): 1559–66. <https://doi.org/10.1002/RCM.5013>.
- Ham, Bryan M., and Aihui MaHam. *Analytical Chemistry : A Chemist and Laboratory Technician's Toolkit*, n.d.
- He, Liqing, Xiaoli Wei, Xipeng Ma, Xinmin Yin, Ming Song, Howard Donninger, Kavitha Yaddanapudi, Craig J. McClain, and Xiang Zhang. “Simultaneous Quantification of Nucleosides and Nucleotides from Biological Samples.” *Journal of the American Society for Mass Spectrometry* 30, no. 6 (June 14, 2019): 987–1000. <https://doi.org/10.1007/S13361-019-02140-7>.
- Heeney, Dustin D., Mélanie G. Gareau, and Maria L. Marco. “Intestinal Lactobacillus in Health and Disease, a Driver or Just along for the Ride?” *Current Opinion in Biotechnology* 49 (February 1, 2018): 140–47. <https://doi.org/10.1016/J.COPBIO.2017.08.004>.
- Huber, Sabrina M., Andrea Leonardi, Peter C. Dedon, and Thomas J. Begley. “The Versatile Roles of the tRNA Epitranscriptome during Cellular Responses to Toxic Exposures and Environmental Stress.” *Toxics* 7, no. 1 (2019). <https://doi.org/10.3390/TOXICS7010017>.
- “Inulin - a Versatile Polysaccharide: Use as Food Chemical and Pharmaceutical Agent | Journal of Excipients and Food Chemicals.” Accessed October 12, 2022. <https://ojs.abo.fi/ojs/index.php/jefc/article/view/40>.

- Jora, Manasses, Andrew P. Burns, Robert L. Ross, Peter A. Lobue, Ruoxia Zhao, Cody M. Palumbo, Peter A. Beal, Balasubrahmanyam Addepalli, and Patrick A. Limbach. “Differentiating Positional Isomers of Nucleoside Modifications by Higher-Energy Collisional Dissociation Mass Spectrometry (HCD MS).” *Journal of the American Society for Mass Spectrometry* 29, no. 8 (2018): 1745–56. <https://doi.org/10.1007/s13361-018-1999-6>.
- Jordan Ontiveros, R., Julian Stoute, and Kathy Fange Liu. “The Chemical Diversity of RNA Modifications.” *The Biochemical Journal* 476, no. 8 (April 26, 2019): 1227–45. <https://doi.org/10.1042/BCJ20180445>.
- Kadumuri, Rajashekar Varma, and Sarath Chandra Janga. “Epitranscriptomic Code and Its Alterations in Human Disease.” *Trends in Molecular Medicine* 24, no. 10 (October 1, 2018): 886–903. <https://doi.org/10.1016/J.MOLMED.2018.07.010>.
- Konno, Masamitsu, Masateru Taniguchi, and Hideshi Ishii. “Significant Epitranscriptomes in Heterogeneous Cancer.” *Cancer Science* 110, no. 8 (2019): 2318–27. <https://doi.org/10.1111/CAS.14095>.
- Lagies, Simon, Manuel Schlimpert, Lukas M. Braun, Michel Kather, Johannes Plagge, Thalia Erbes, Uwe A. Wittel, and Bernd Kammerer. “Unraveling Altered RNA Metabolism in Pancreatic Cancer Cells by Liquid-Chromatography Coupling to Ion Mobility Mass Spectrometry.” *Analytical and Bioanalytical Chemistry* 411, no. 24 (2019): 6319–28. <https://doi.org/10.1007/s00216-019-01814-1>.
- Lauman, Richard, and Benjamin A. Garcia. “Unraveling the RNA Modification Code with Mass Spectrometry.” *Molecular Omics* 16, no. 4 (August 1, 2020): 305–15. <https://doi.org/10.1039/C8MO00247A>.

Lebeer, Sarah, Peter A. Bron, Maria L. Marco, Jan Peter Van Pijkeren, Mary O’Connell

Motherway, Colin Hill, Bruno Pot, Stefan Roos, and Todd Klaenhammer. “Identification of Probiotic Effector Molecules: Present State and Future Perspectives.” *Current Opinion in Biotechnology* 49 (February 1, 2018): 217–23.

<https://doi.org/10.1016/J.COPBIO.2017.10.007>.

Lehman, Niles. “RNA in Evolution.” *Wiley Interdisciplinary Reviews: RNA* 1, no. 2 (September 1, 2010): 202–13. <https://doi.org/10.1002/WRNA.37>.

Lewis, Cole J.T., Tao Pan, and Auinash Kalsotra. “RNA Modifications and Structures Cooperate to Guide RNA-Protein Interactions.” *Nature Reviews. Molecular Cell Biology* 18, no. 3 (March 1, 2017): 202–10. <https://doi.org/10.1038/NRM.2016.163>.

Li, Siwei, and Patrick A. Limbach. “Identification of RNA Sequence Isomer by Isotope Labeling and LC-MS/MS.” *Journal of Mass Spectrometry : JMS* 49, no. 11 (November 1, 2014): 1191–98. <https://doi.org/10.1002/JMS.3449>.

Li, Xiaoyu, Xushen Xiong, and Chengqi Yi. “Epitranscriptome Sequencing Technologies: Decoding RNA Modifications.” *Nature Methods*. Nature Publishing Group, December 29, 2016. <https://doi.org/10.1038/nmeth.4110>.

Licht, Konstantin, and Michael F. Jantsch. “Rapid and Dynamic Transcriptome Regulation by RNA Editing and RNA Modifications.” *The Journal of Cell Biology* 213, no. 1 (April 1, 2016): 15–22. <https://doi.org/10.1083/JCB.201511041>.

Livneh, Ido, Sharon Moshitch-Moshkovitz, Ninette Amariglio, Gideon Rechavi, and Dan Dominianni. “The m⁶A Epitranscriptome: Transcriptome Plasticity in Brain Development and Function.” *Nature Reviews. Neuroscience* 21, no. 1 (January 1, 2020): 36–51. <https://doi.org/10.1038/S41583-019-0244-Z>.

- Nachtergaele, Sigrid, and Chuan He. "Chemical Modifications in the Life of an mRNA Transcript." *Annual Review of Genetics* 52 (November 23, 2018): 349–72.
<https://doi.org/10.1146/ANNUREV-GENET-120417-031522>.
- Neffling, Milla Riina, Lisa Spoof, Michael Quilliam, and Jussi Meriluoto. "LC-ESI-Q-TOF-MS for Faster and Accurate Determination of Microcystins and Nodularins in Serum." *Journal of Chromatography. B, Analytical Technologies in the Biomedical and Life Sciences* 878, no. 26 (September 2010): 2433–41. <https://doi.org/10.1016/J.JCHROMB.2010.07.018>.
- Pan, Tao. "Modifications and Functional Genomics of Human Transfer RNA." *Cell Research* 28, no. 4 (April 1, 2018): 395–404. <https://doi.org/10.1038/S41422-018-0013-Y>.
- Ranjan, Namit, and Sebastian A. Leidel. "The Epitranscriptome in Translation Regulation: mRNA and tRNA Modifications as the Two Sides of the Same Coin?" *FEBS Letters* 593, no. 13 (July 1, 2019): 1483–93. <https://doi.org/10.1002/1873-3468.13491>.
- Rose, Rebecca E., Ryan Quinn, Jackie L. Sayre, and Daniele Fabris. "Profiling Ribonucleotide Modifications at Full-Transcriptome Level: A Step toward MS-Based Epitranscriptomics." *RNA (New York, N.Y.)* 21, no. 7 (July 1, 2015): 1361–74.
<https://doi.org/10.1261/RNA.049429.114>.
- . "Profiling Ribonucleotide Modifications at Full-Transcriptome Level: A Step toward MS-Based Epitranscriptomics." *Rna* 21, no. 7 (2015): 1361–74.
<https://doi.org/10.1261/rna.049429.114>.
- Rosenow, Carsten, Rini Mukherjee Saxena, Mark Durst, and Thomas R. Gingeras. "Prokaryotic RNA Preparation Methods Useful for High Density Array Analysis: Comparison of Two Approaches." *Nucleic Acids Research* 29, no. 22 (2001).
<https://doi.org/10.1093/NAR/29.22.E112>.

- Saletore, Yogesh, Kate Meyer, Jonas Korlach, Igor D. Vilfan, Samie Jaffrey, and Christopher E. Mason. “The Birth of the Epitranscriptome: Deciphering the Function of RNA Modifications.” *Genome Biology* 13, no. 10 (October 31, 2012): 175.
<https://doi.org/10.1186/GB-2012-13-10-175/FIGURES/5>.
- Schwartz, Schraga, and Yuri Motorin. “Next-Generation Sequencing Technologies for Detection of Modified Nucleotides in RNAs.” *RNA Biology* 14, no. 9 (2017): 1124–37.
<https://doi.org/10.1080/15476286.2016.1251543>.
- Shi, Hailing, Jiangbo Wei, and Chuan He. “Where, When, and How: Context-Dependent Functions of RNA Methylation Writers, Readers, and Erasers.” *Molecular Cell* 74, no. 4 (May 16, 2019): 640–50. <https://doi.org/10.1016/J.MOLCEL.2019.04.025>.
- Silantsev, Artemiy S., Luca Falzone, Massimo Libra, Olga I. Gurina, Karina Sh Kardashova, Taxiarchis K. Nikolouzakis, Alexander E. Nosyrev, Christopher W. Sutton, Panayiotis D. Mitsias, and Aristides Tsatsakis. “Current and Future Trends on Diagnosis and Prognosis of Glioblastoma: From Molecular Biology to Proteomics.” *Cells* 8, no. 8 (2019).
<https://doi.org/10.3390/cells8080863>.
- Su, Dan, Clement T. Y. Chan, Chen Gu, Kok Seong Lim, Yok Hian Chionh, Megan E. McBee, Brandon S. Russell, I. Ramesh Babu, Thomas J. Begley, and Peter C. Dedon. “Quantitative Analysis of Ribonucleoside Modifications in tRNA by HPLC-Coupled Mass Spectrometry.” *Nature Protocols* 9, no. 4 (2014): 828–41.
<https://doi.org/10.1038/nprot.2014.047>.
- Swanson, Kelly S., Glenn R. Gibson, Robert Hutkins, Raylene A. Reimer, Gregor Reid, Kristin Verbeke, Karen P. Scott, et al. “The International Scientific Association for Probiotics and Prebiotics (ISAPP) Consensus Statement on the Definition and Scope of Synbiotics.”

Nature Reviews Gastroenterology & Hepatology 2020 17:11 17, no. 11 (August 21, 2020): 687–701. <https://doi.org/10.1038/s41575-020-0344-2>.

Yanas, Amber, and Kathy Fange Liu. “RNA Modifications and the Link to Human Disease.” *Methods in Enzymology* 626 (January 1, 2019): 133–46. <https://doi.org/10.1016/BS.MIE.2019.08.003>.

Zaccara, Sara, Ryan J. Ries, and Samie R. Jaffrey. “Reading, Writing and Erasing MRNA Methylation.” *Nature Reviews Molecular Cell Biology* 2019 20:10 20, no. 10 (September 13, 2019): 608–24. <https://doi.org/10.1038/s41580-019-0168-5>.

Zhu, Yuanting, Jinxin Liu, Julian M. Lopez, and David A. Mills. “Inulin Fermentation by Lactobacilli and Bifidobacteria from Dairy Calves.” *Applied and Environmental Microbiology* 87, no. 1 (January 1, 2021): 1–12. <https://doi.org/10.1128/AEM.01738-20>.